Scientific Revolutions and Visual Evidence in Science

Otávio Bueno

Department of Philosophy

University of Miami

Coral Gables, FL 33124

E-mail: otaviobueno@me.com

Thomas Kuhn

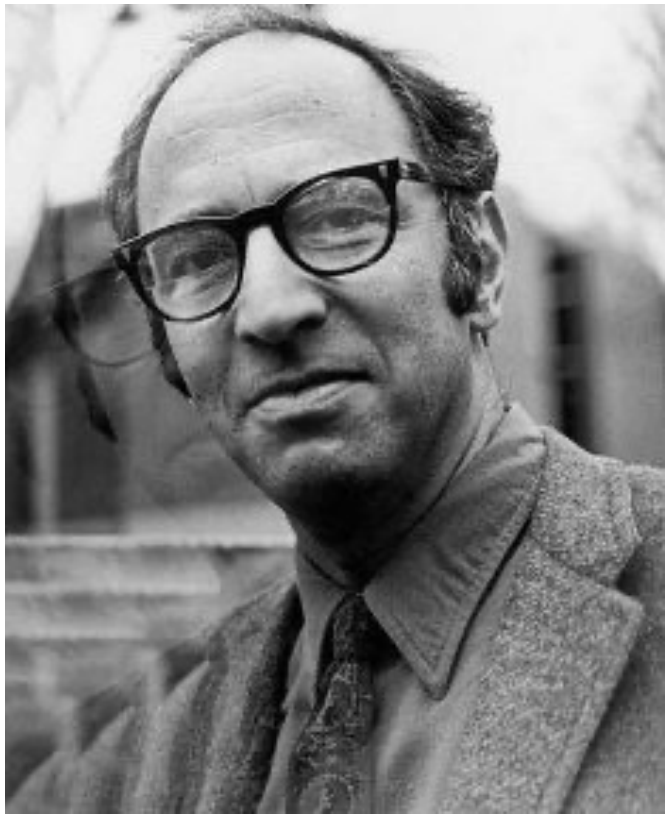

Kuhn, paradigms, and normal science

Paradigm

- Aims
- Methods
- Theories

Normal Science

The Structure of Scientific Revolutions

Paradigm$_1$				**Paradigm$_2$**
• Aims	→	*Anomalies* + *Crisis*	→	Aims$_2$
• Methods				Methods$_2$
• Theories				Theories$_2$

Normal Science	→	*Revolutionary Science*	→	New normal science

- *Some traits*: incommensurability between different paradigms.
- *Difficulties*: Relativism? Scientific progress? Scientific irrationality?

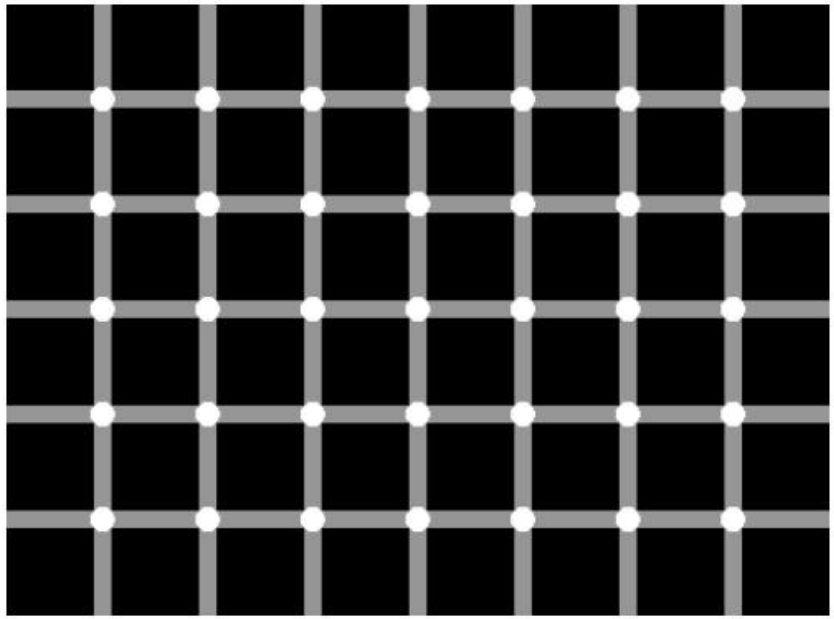

Count the black dots! :o)

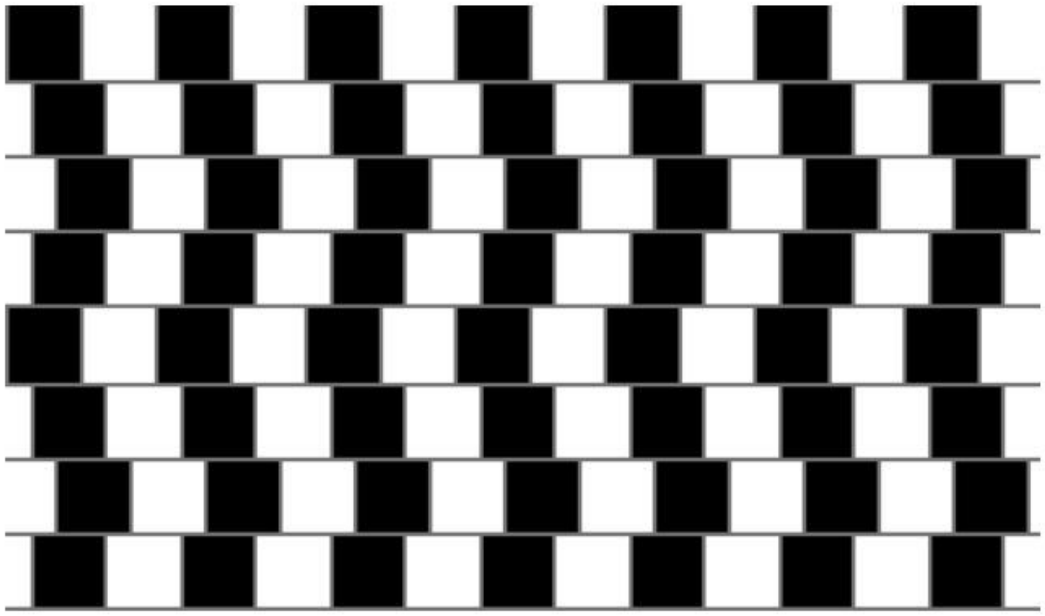

Are the horizontal lines parallel or do they slope?

Look at the chart and say the COLOUR not the word

YELLOW BLUE ORANGE
BLACK RED GREEN
PURPLE YELLOW RED
ORANGE GREEN BLACK
BLUE RED PURPLE
GREEN BLUE ORANGE

Left – Right Conflict

Your right brain tries to say the colour but your left brain insists on reading the word.

Perception

- An important feature of perception is that it satisfies two conditions:
- (C1) Had the scene before our eyes been different (within the sensitivity range of our eyes), our perceptual experience would have been correspondingly different.
- (C2) Had the scene before our eyes been the same (within the sensitivity range of our eyes), our perceptual experience would have been correspondingly the same.

Evidence

- We have *evidence* for a state of affairs *S* when there are good reasons to believe that *S* is the case, and these reasons are such that:
- (i) they make *S* more likely than *non-S*;
- (ii) they rule out those items that are compatible with *non-S* being the case.

Visual Evidence

We have *visual evidence* for a state of affairs *S* if:

- (i) we have evidence for *S*, and
- (ii) the evidence is visually based.

A piece of evidence is *visually based* if:

- (C1) Had the sample been different (within the sensitivity range of the relevant instruments), the image produced would have been correspondingly different.
- (C2) Had the sample been the same (within the sensitivity range of the relevant instruments), the image produced would have been correspondingly the same.


Photo: LEO Electron Microscopy Ltd

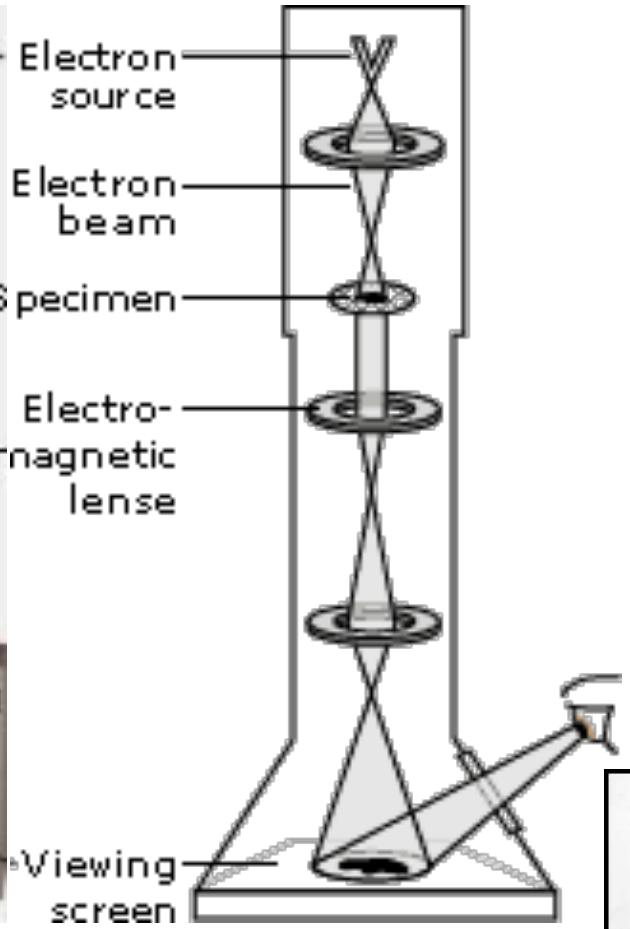
Electron source
Electron beam
Specimen
Electro-magnetic lense
Viewing screen

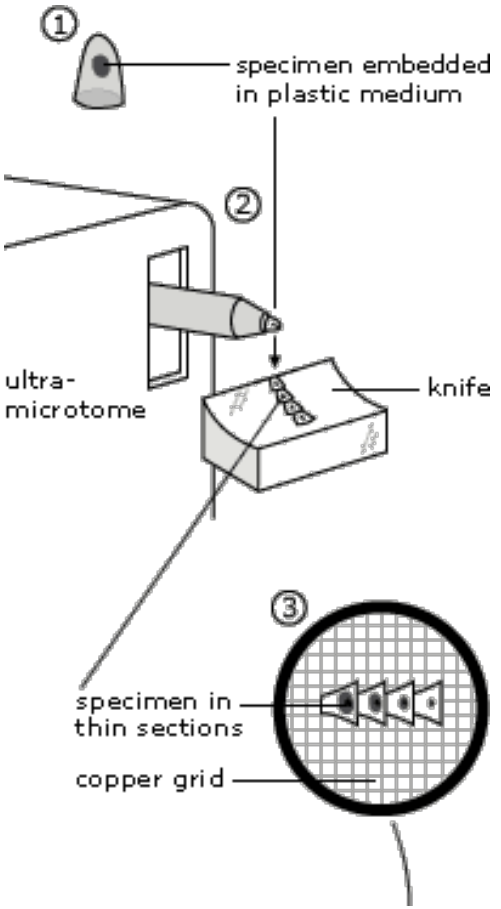
1
specimen embedded in plastic medium
2
ultra-microtome
knife
3
specimen in thin sections
copper grid

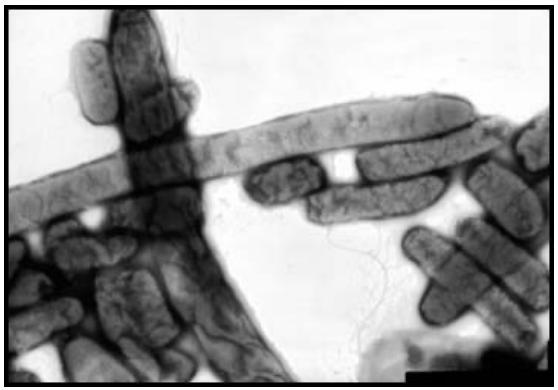

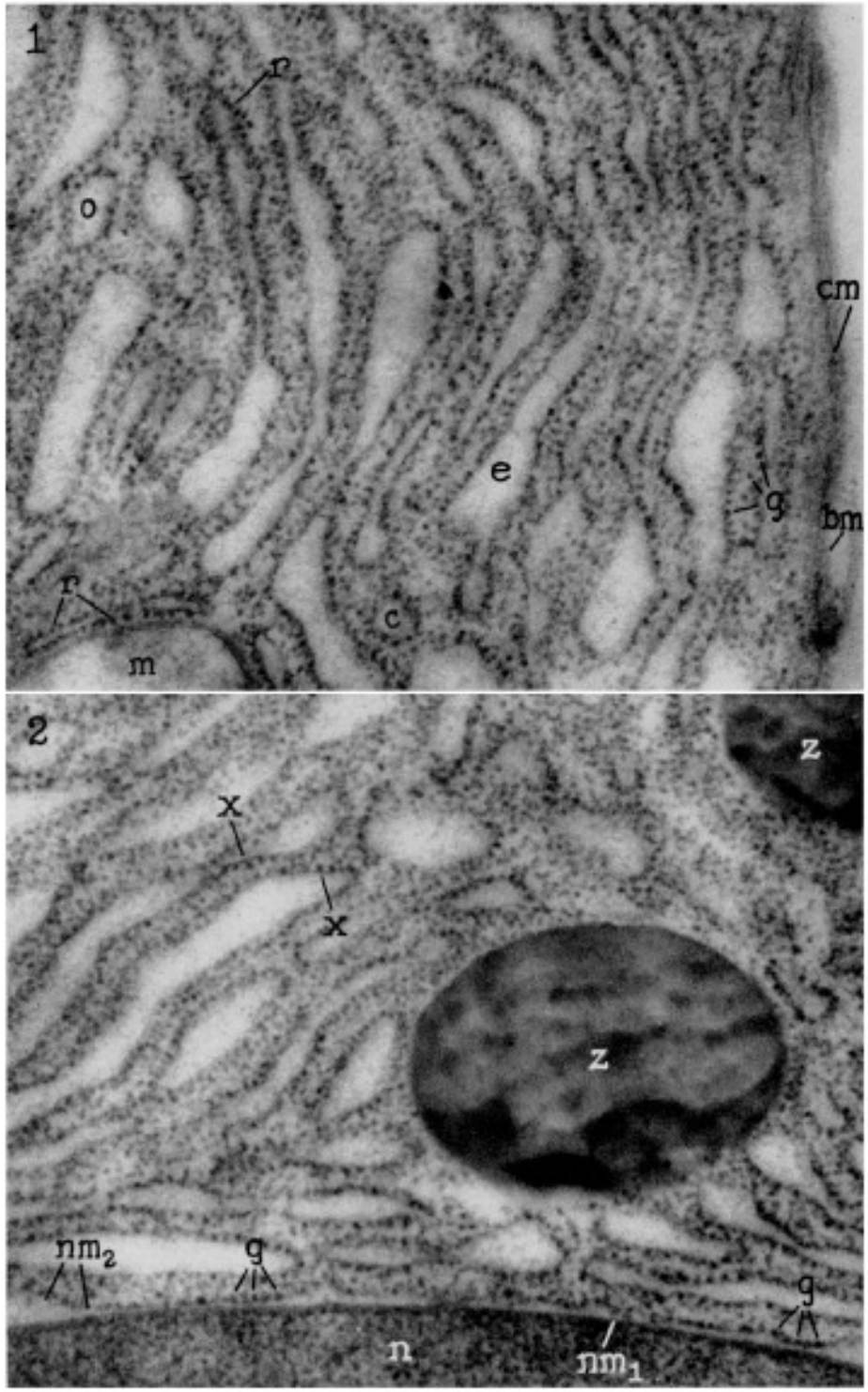
1
r
o
cm
e
g
bm
r
c
m
2
z
x
x
z
nm2
g
g
n
nm1

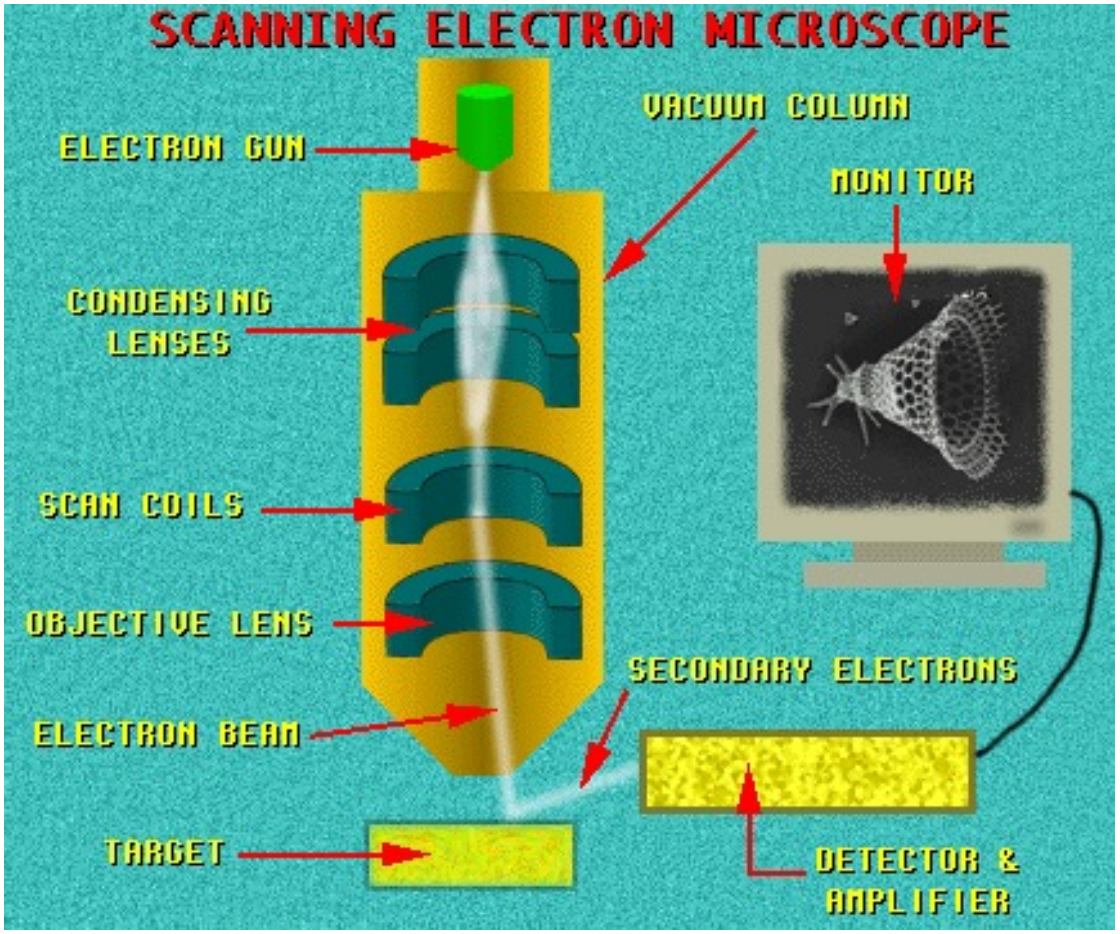
SCANNING ELECTRON MICROSCOPE
ELECTRON GUN
VACUUM COLUMN
MONITOR
CONDENSING LENSES
SCAN COILS
OBJECTIVE LENS
SECONDARY ELECTRONS
ELECTRON BEAM
TARGET
DETECTOR & AMPLIFIER

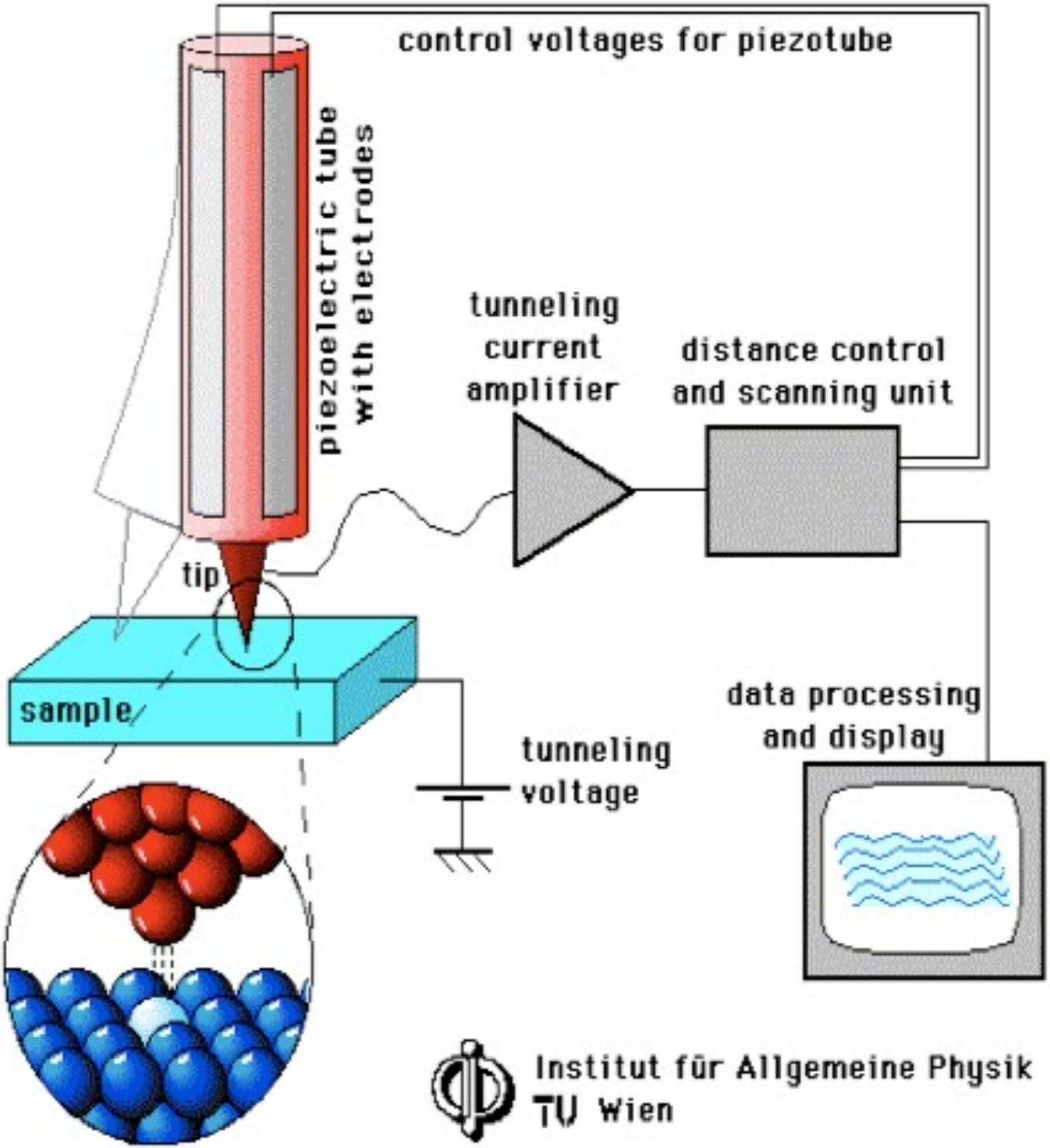
control voltages for piezotube
piezoelectric tube with electrodes
tunneling current amplifier
distance control and scanning unit
tip
sample
tunneling voltage
data processing and display
Institut für Allgemeine Physik
TU Wien

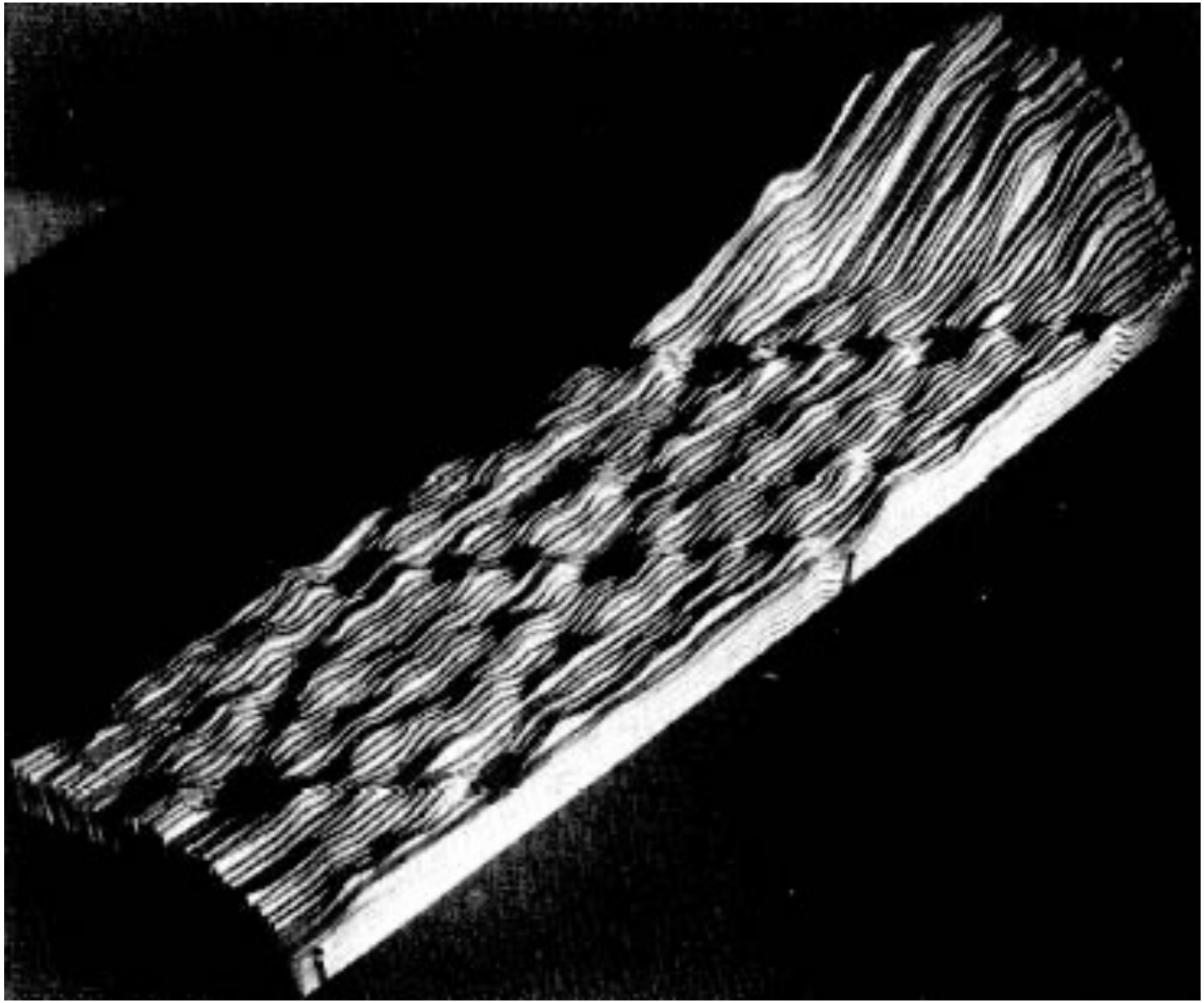

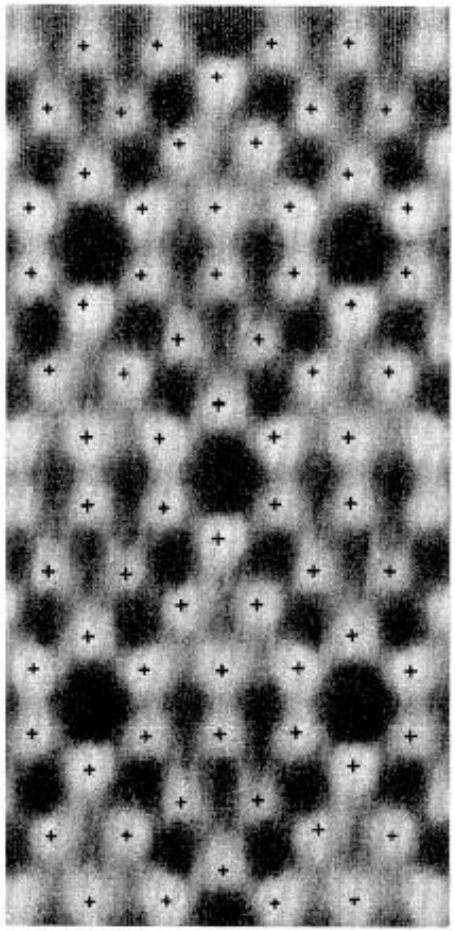

FIG. 2. Top view of the relief shown in Fig. 1 (the hill at the right is not included) clearly exhibiting the sixfold rotational symmetry of the maxima around the rhombohedron corners. Brightness is a measure of the altitude, but is not to scale. The crosses indicate adatom positions of the modified adatom model (see Fig. 3) or "milk-stool" positions (Ref. 5).

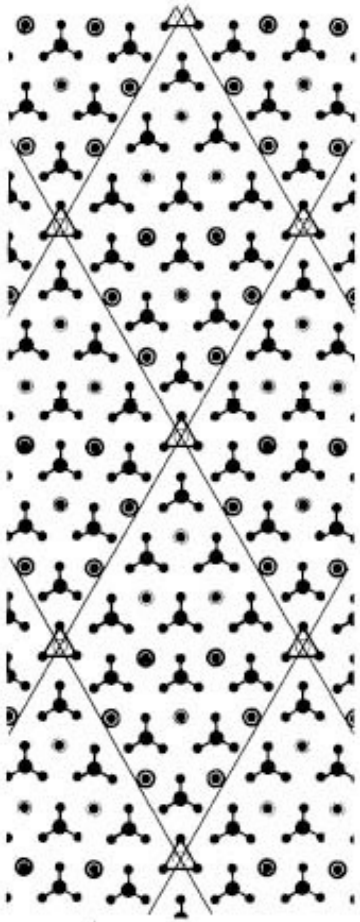

FIG. 3. Modified adatom model. The underlying top-layer atom positions are shown by dots, and the rest atoms with unsatisfied dangling bonds carry circles, whose thickness indicates the depth measured as discussed in the text. The adatoms are represented by large dots with corresponding bonding arms. The empty potential adatom position is indicated by an empty circle in the triangle of adjacent rest atoms. The grid indicates the 7×7 unit cells.

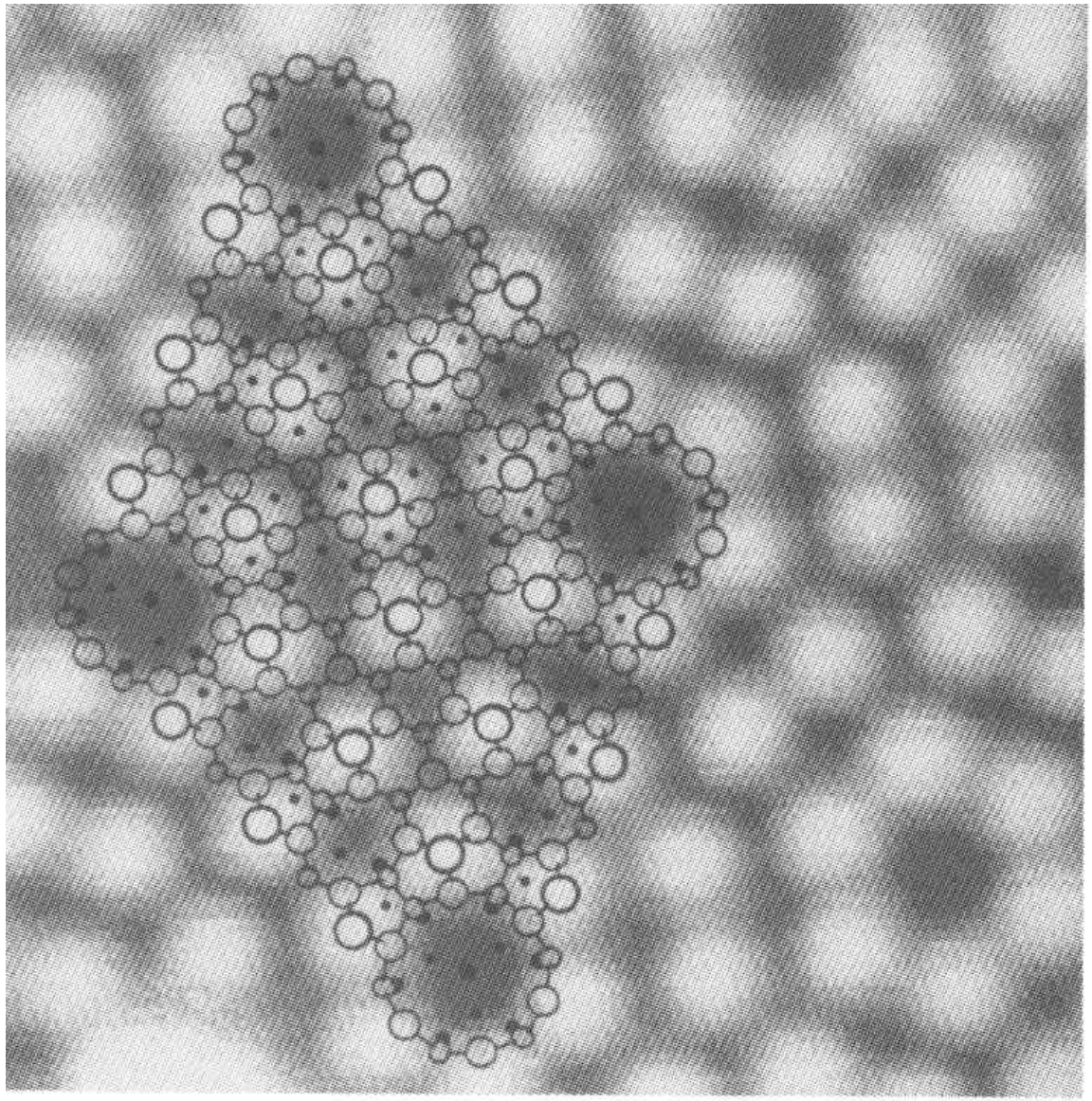

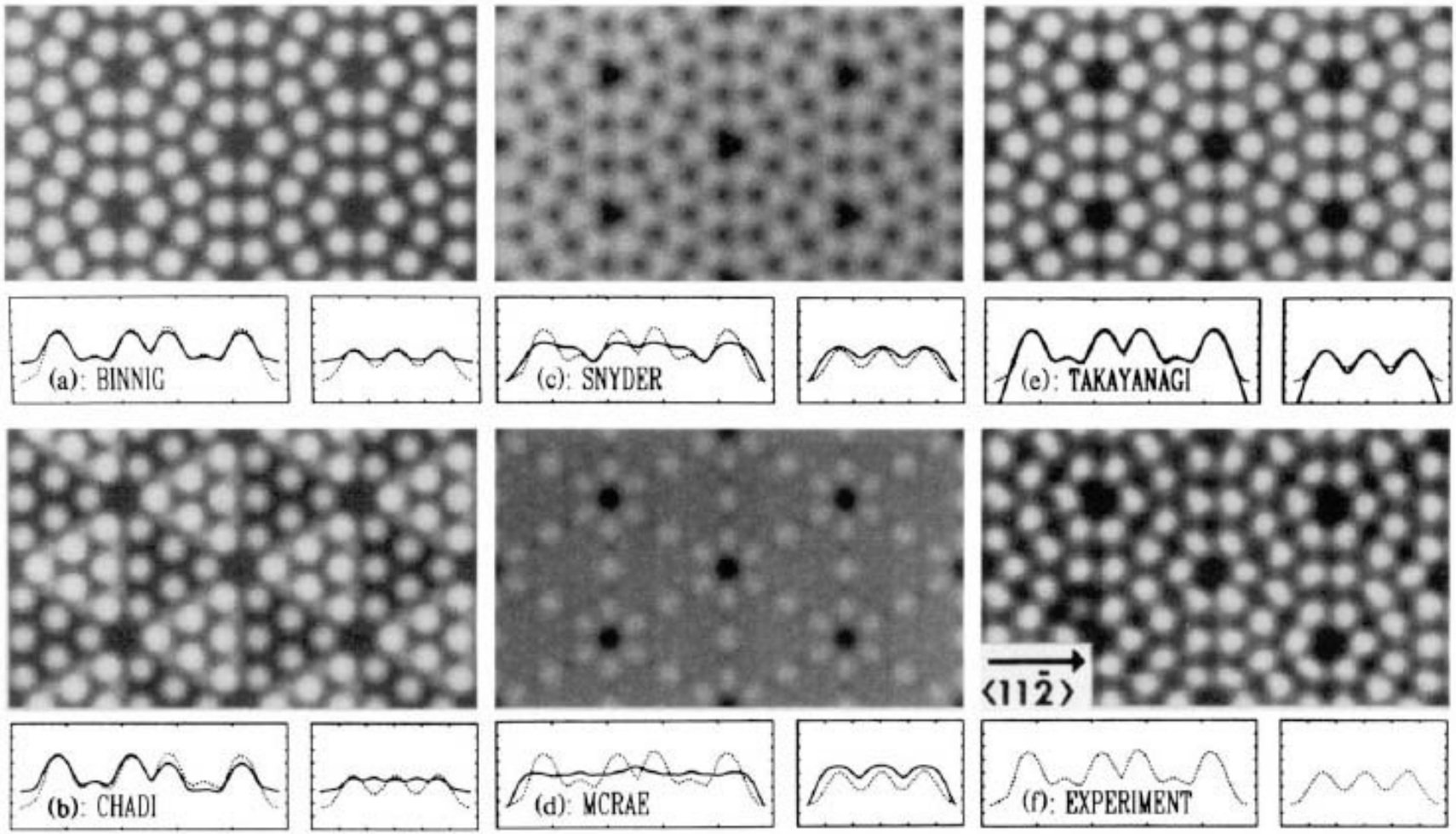

FIG. 2. (a)–(e) STM images calculated for (a) Binnig's model, (b) Chadi's model, (c) Snyder's model, (d) McRae's model, and (e) Takayanagi's model. (f) Measured STM image. The line scans run from corner hole to corner hole along the long (left) and short (right) diagonal of the (7×7) unit cell. The vertical range in these line scans is 4 Å. Solid lines are calculations, dashed lines represent the experimental results.

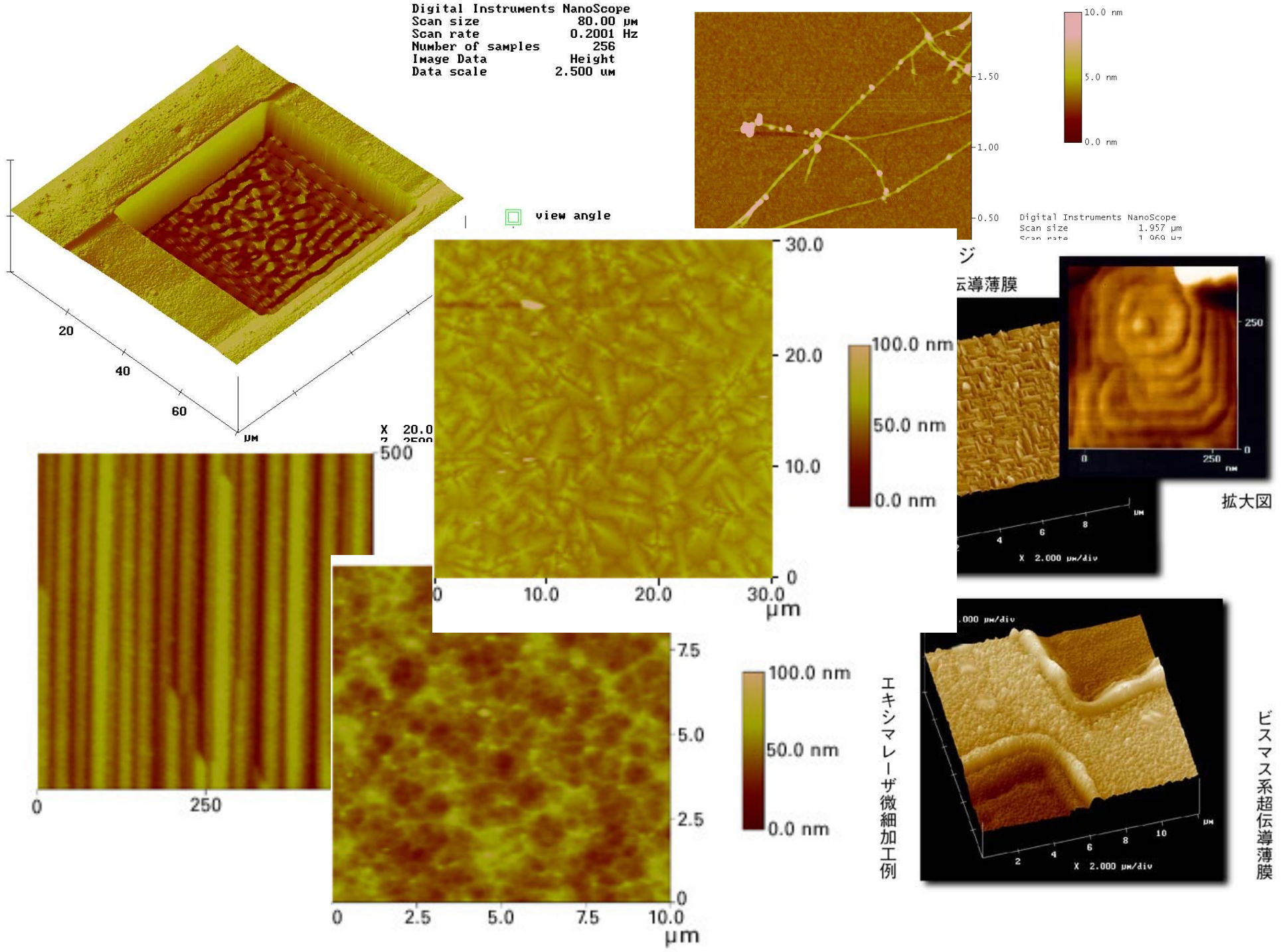
Digital Instruments NanoScope
Scan size 80.00 µm
Scan rate 0.2001 Hz
Number of samples 256
Image Data Height
Data scale 2.500 um
view angle
20
40
60
µm
10.0 nm
5.0 nm
0.0 nm
1.50
1.00
0.50
Digital Instruments NanoScope
Scan size 1.957 µm
ジ
伝導薄膜
拡大図
X 2.000 µm/div
30.0
20.0
10.0
0
100.0 nm
50.0 nm
0.0 nm
X 20.0
500
250
7.5
5.0
2.5
エキシマレーザ微細加工例
X 2.000 µm/div
ビスマス系超伝導薄膜

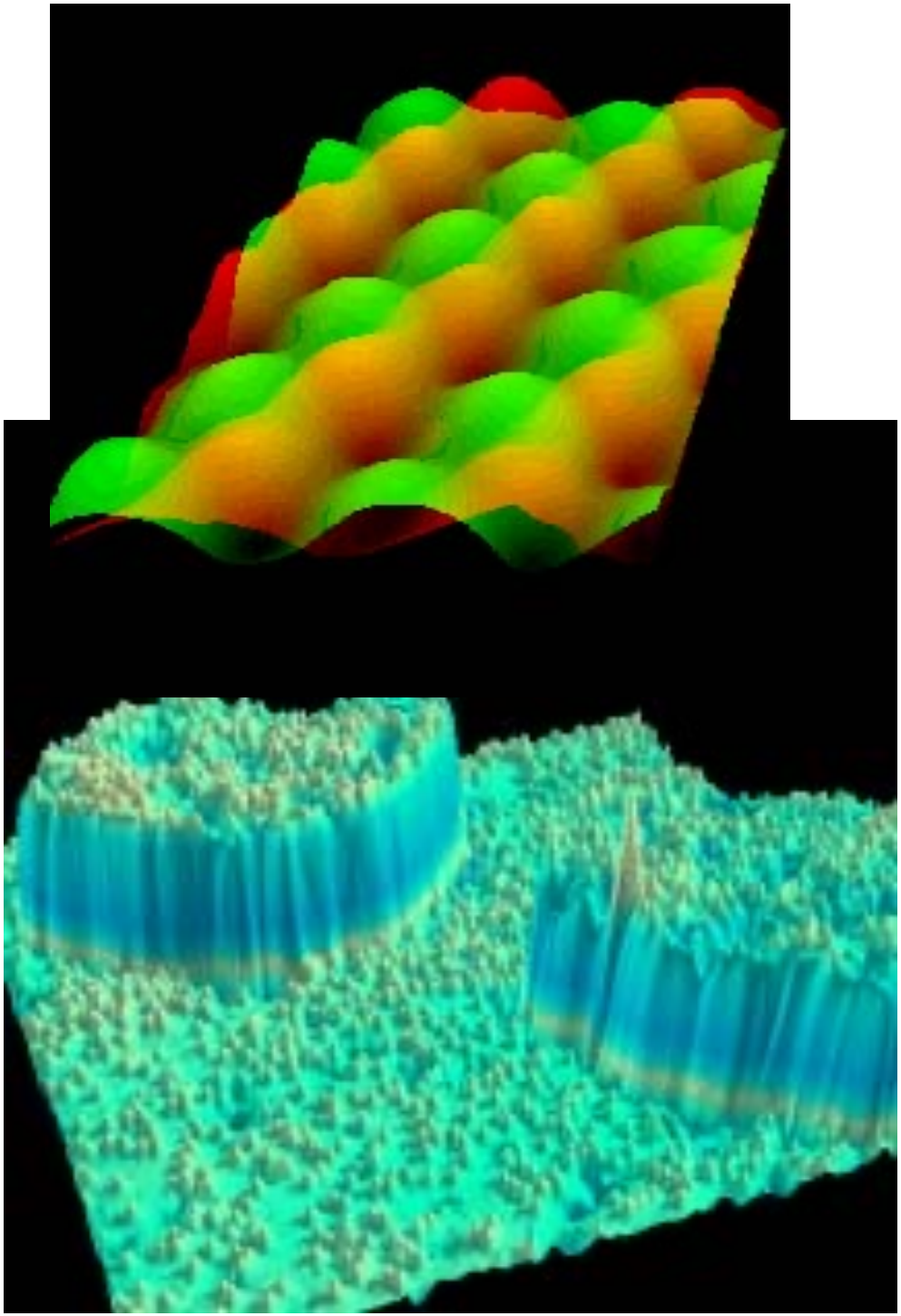

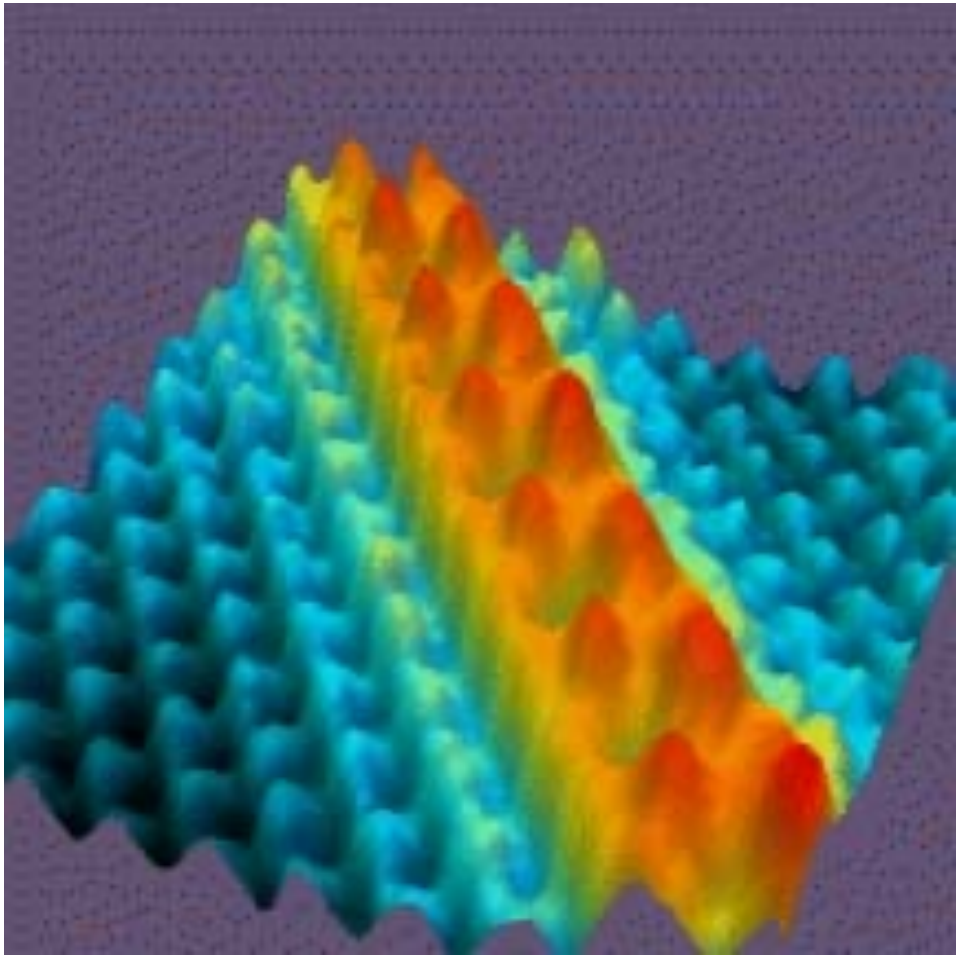

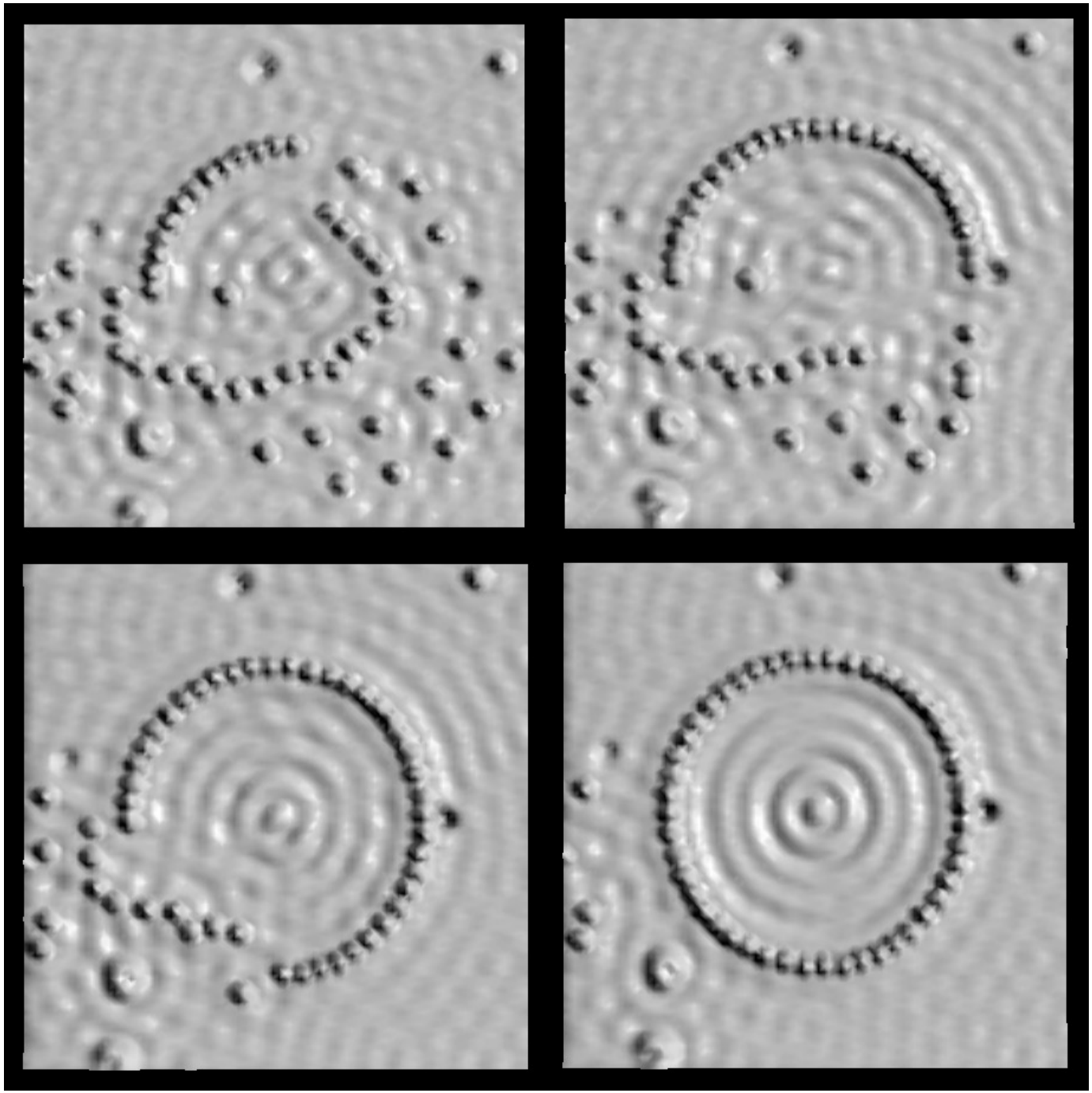

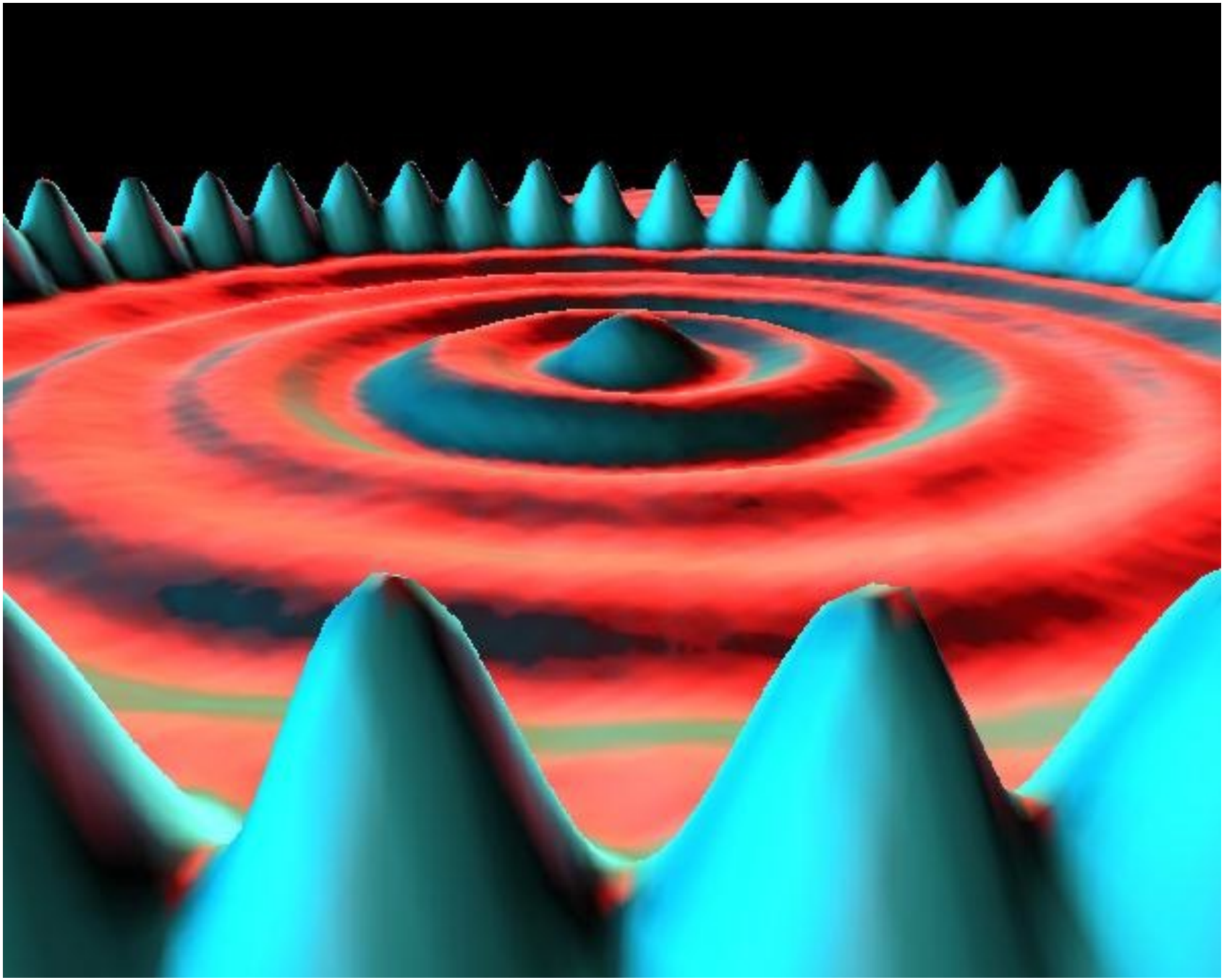

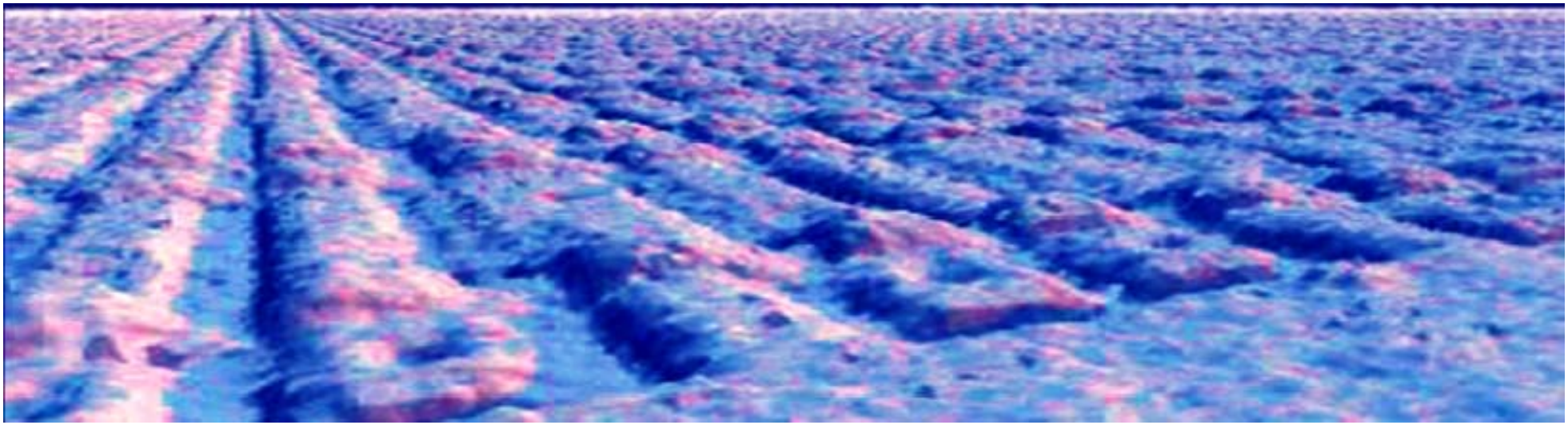

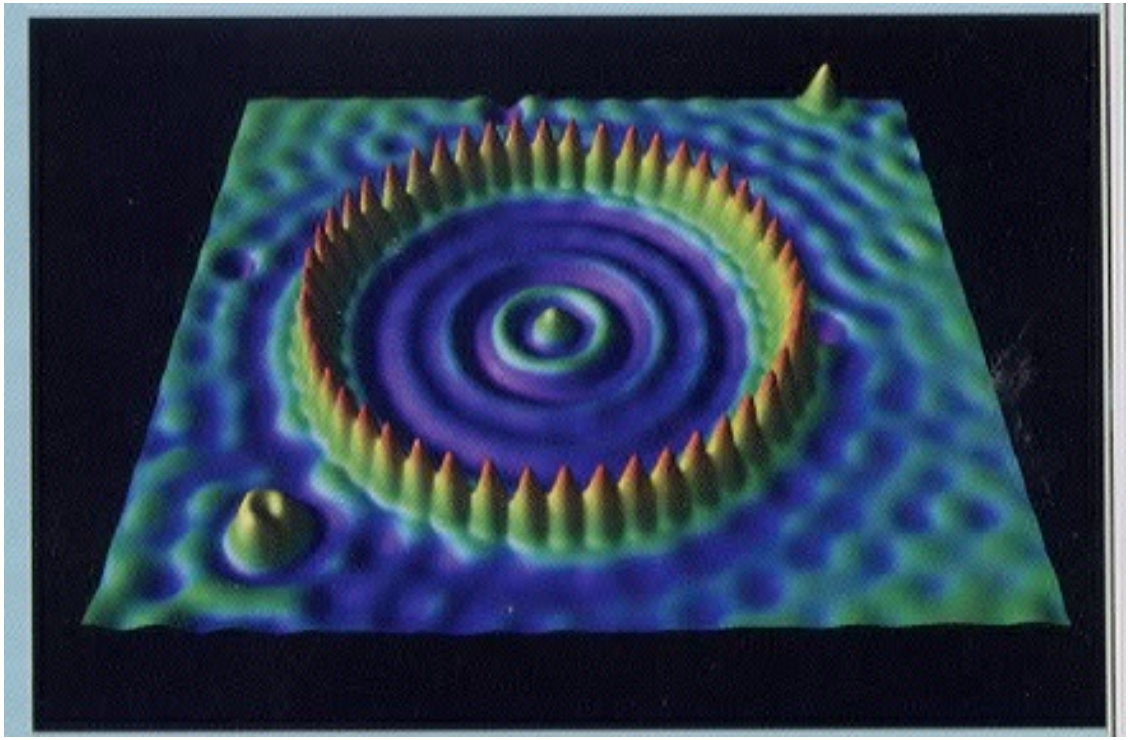

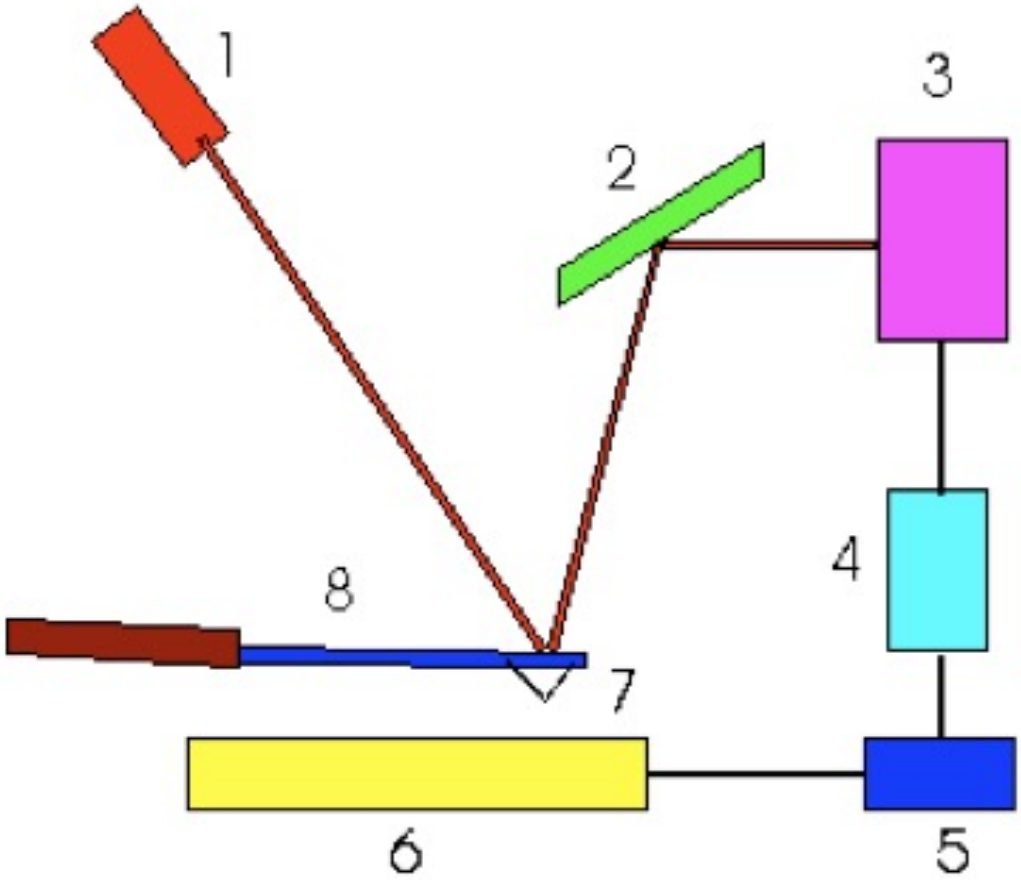

1. Laser
2. Mirror
3. Photodetector
4. Amplifier
5. Register
6. Sample
7. Probe
8. Cantilever

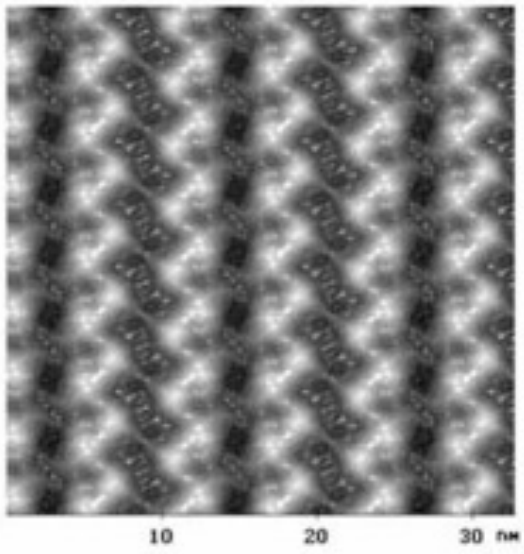

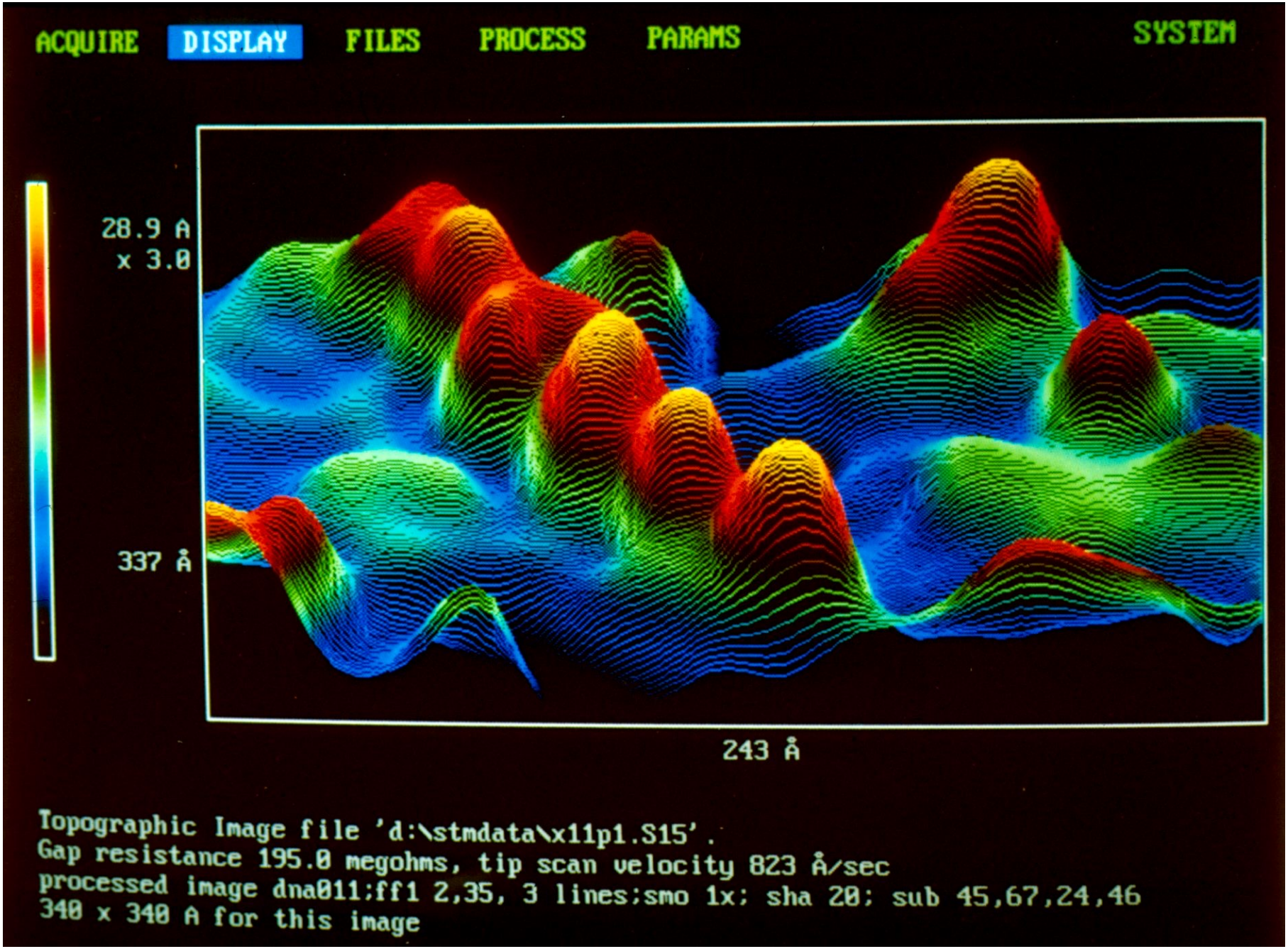
ACQUIRE
DISPLAY
FILES
PROCESS
PARAMS
SYSTEM
28.9 A
x 3.0
337 Å
243 Å
Topographic Image file 'd:\stmdata\x11p1.S15'.
Gap resistance 195.0 megohms, tip scan velocity 823 Å/sec
processed image dna011;ff1 2,35, 3 lines;smo 1x; sha 20; sub 45,67,24,46
340 x 340 A for this image

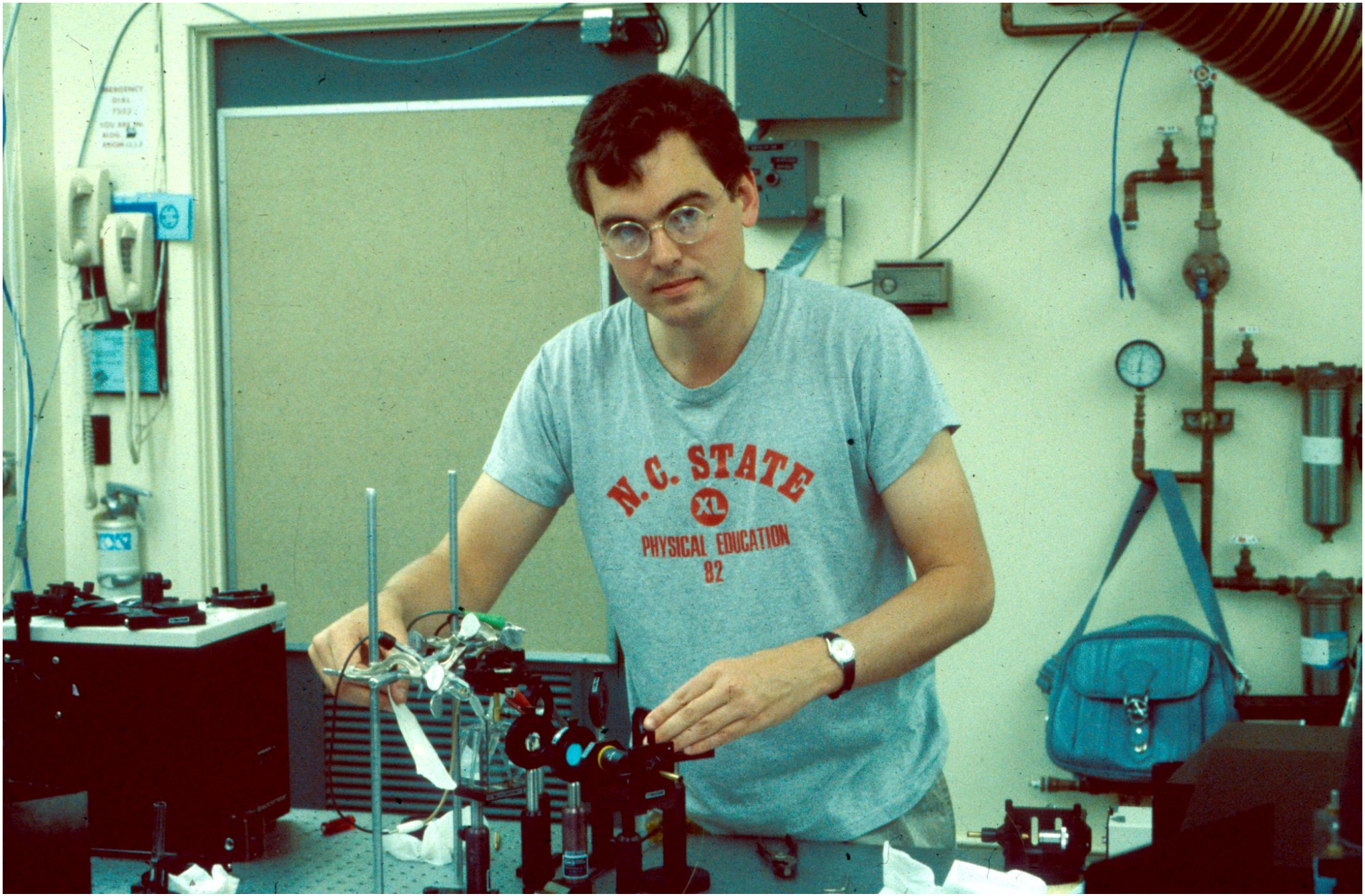
N.C. STATE
XL
PHYSICAL EDUCATION
82

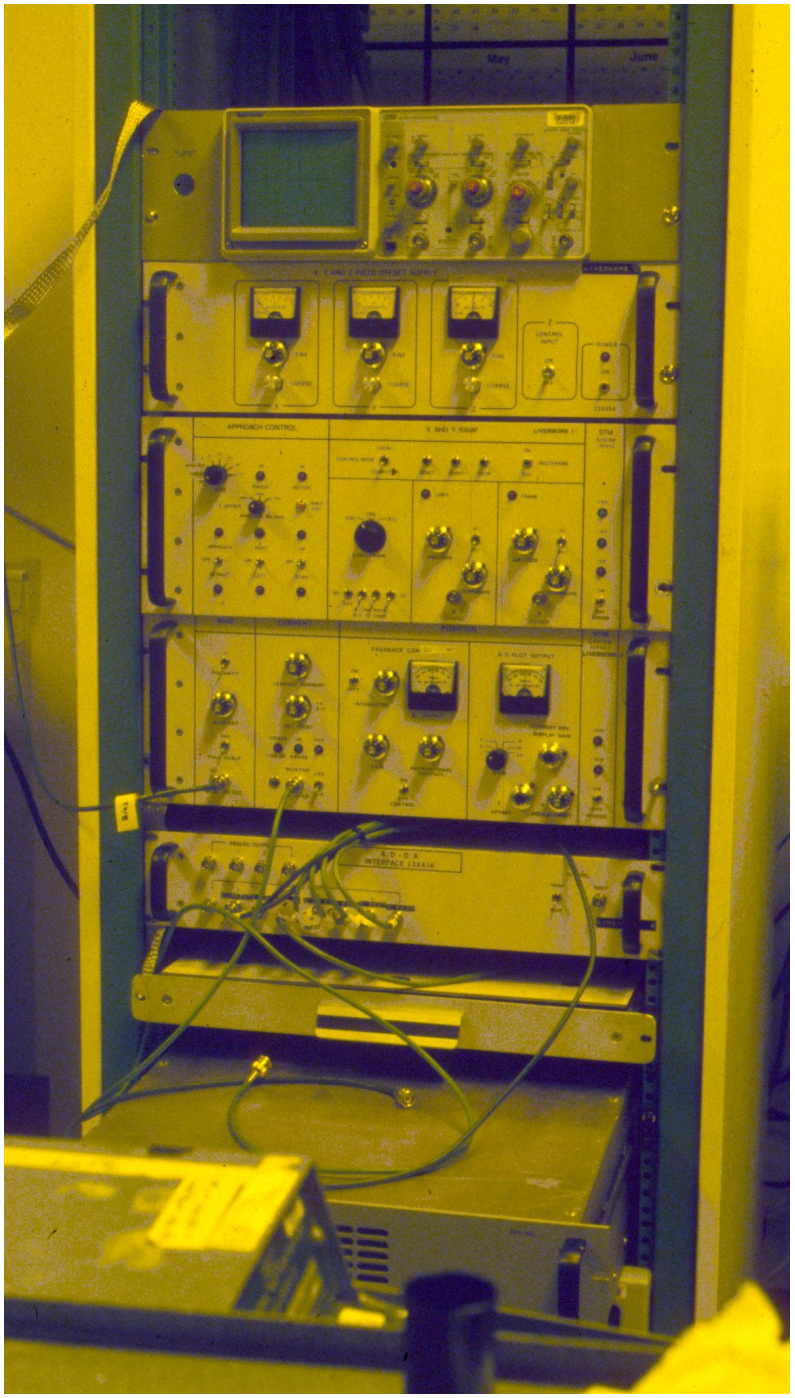
May
June
APPROACH CONTROL
X AND Y RAMP
A/D - D/A
INTERFACE 134414

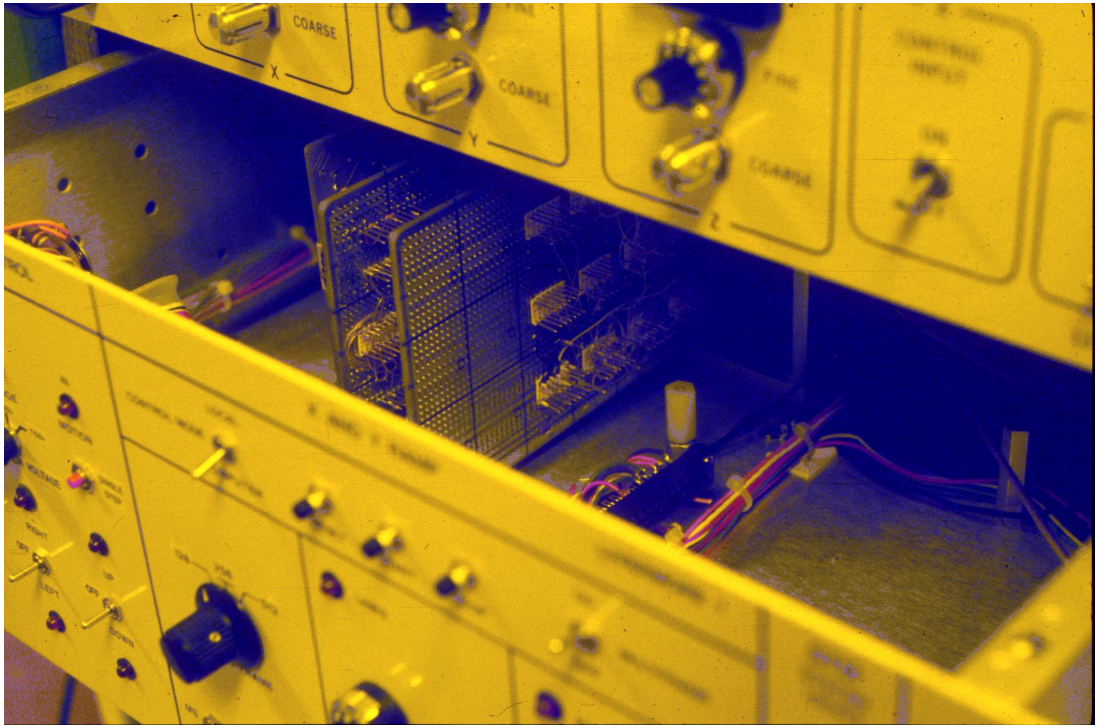
COARSE
X
COARSE
Y
Z

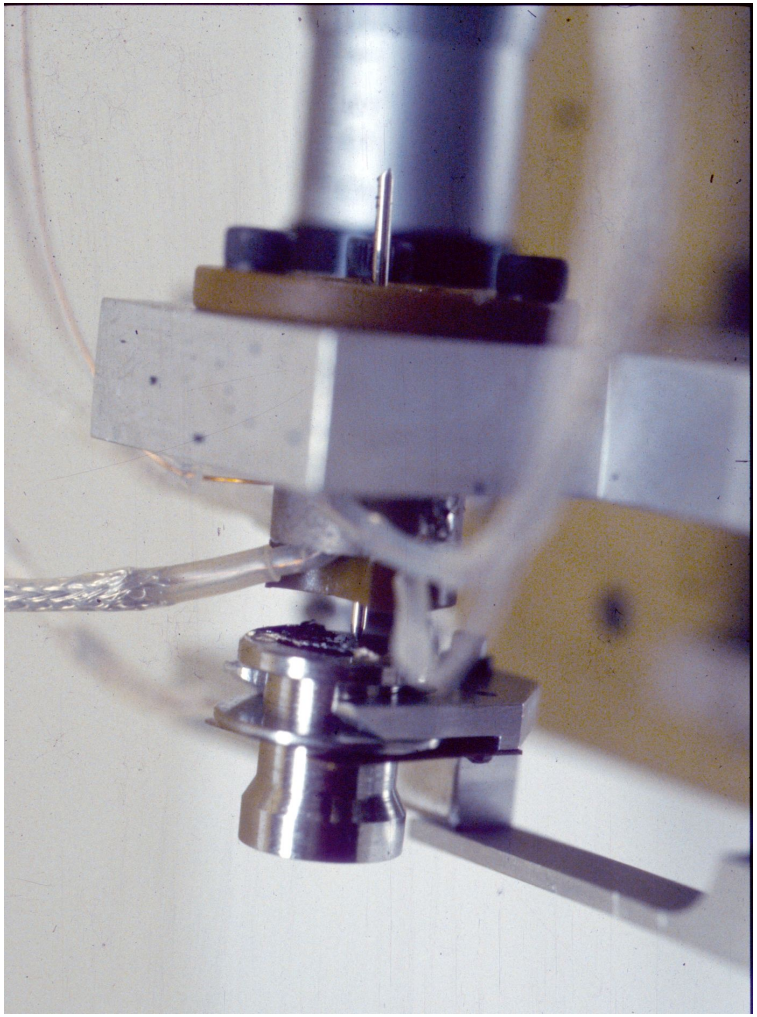

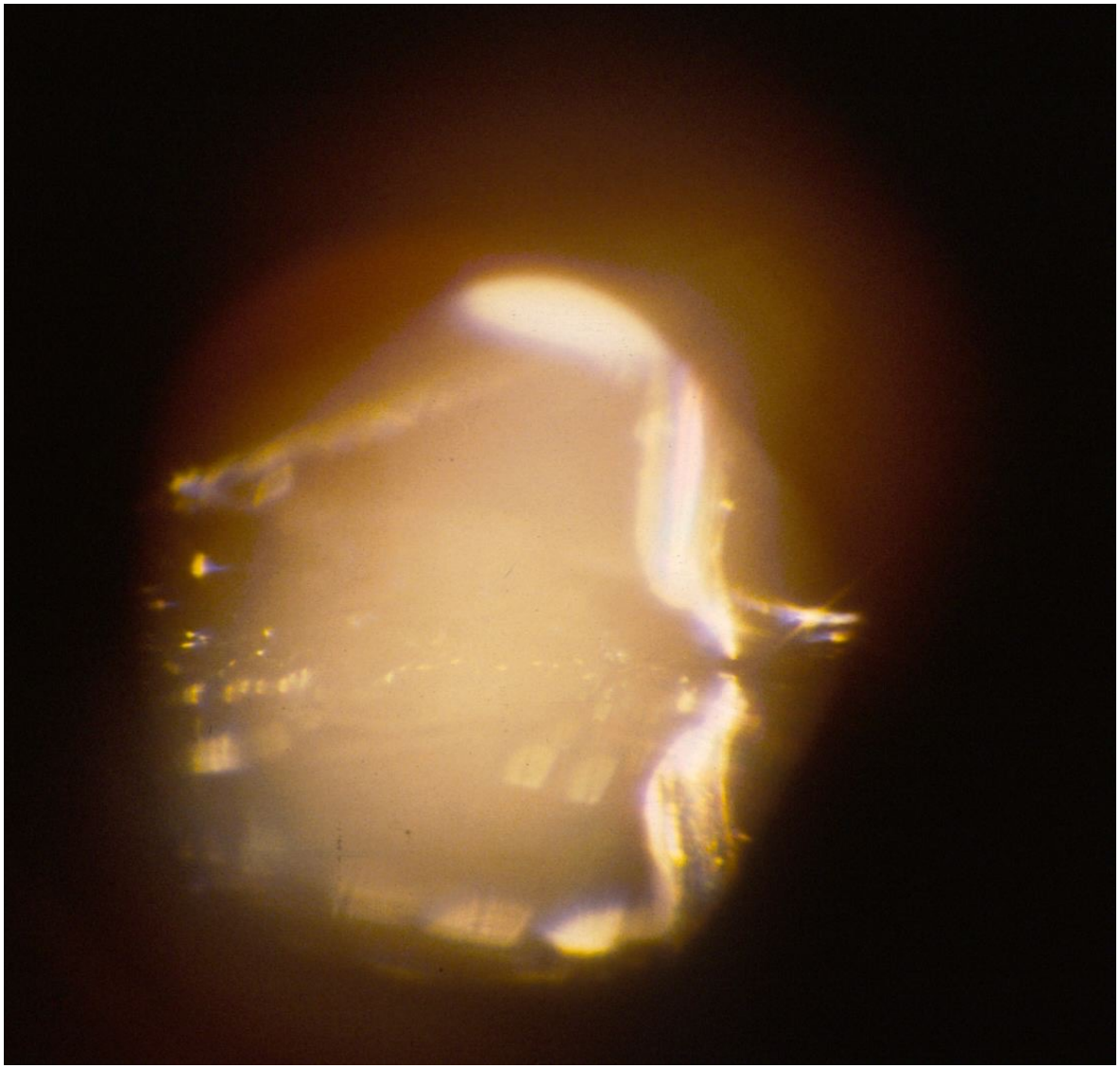

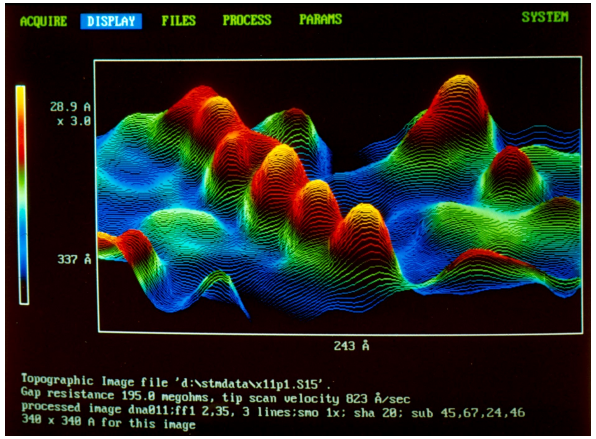
ACQUIRE
DISPLAY
FILES
PROCESS
PARAMS
SYSTEM
28.9 Å
x 3.0
337 Å
243 Å
Topographic Image file 'd:\stmdata\x11p1.815'.
Gap resistance 195.0 megohms, tip scan velocity 823 Å/sec
processed image dna011:ff1 2,35, 3 lines;smo 1x; sha 20; sub 45,67,24,46
340 x 340 Å for this image

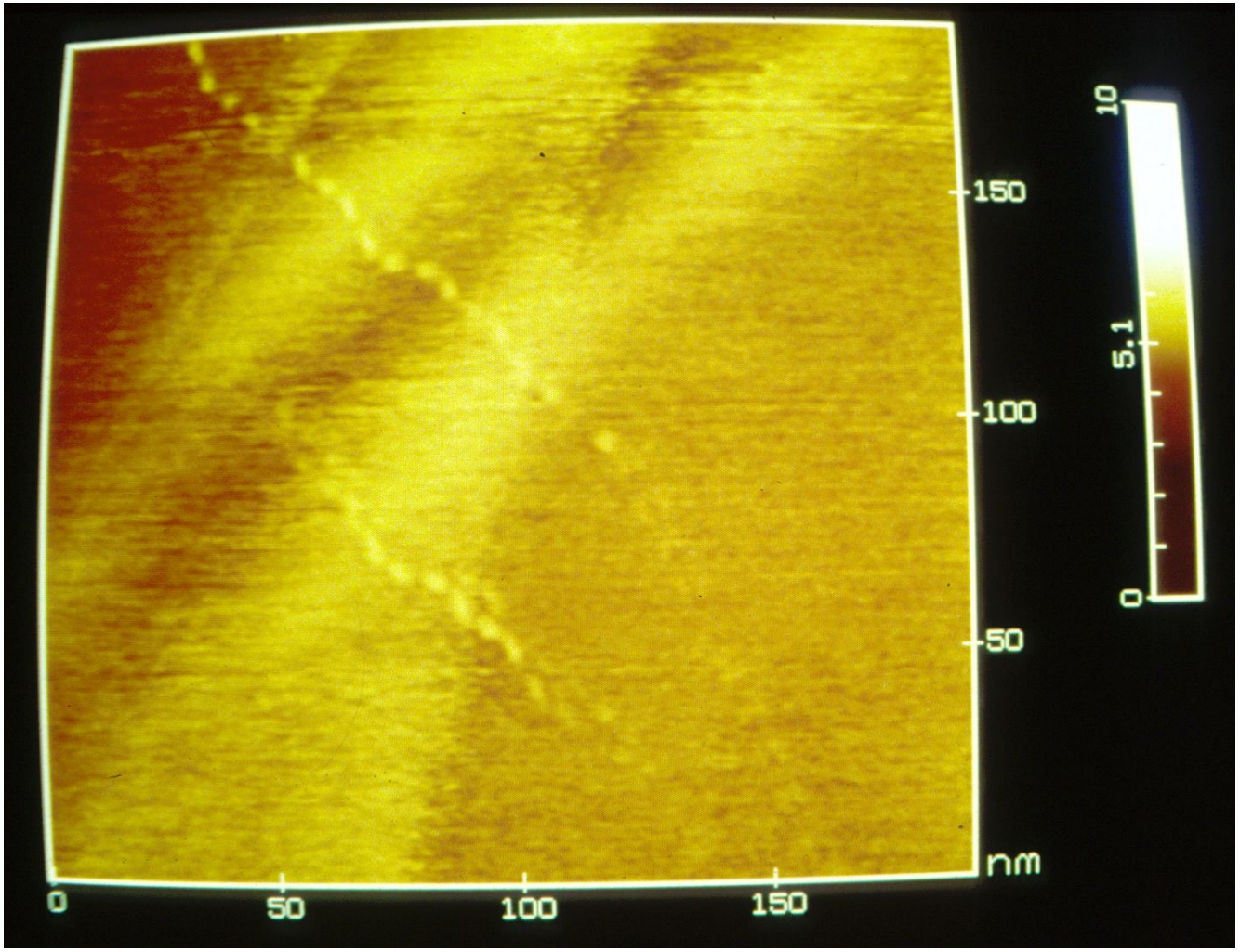
10
5.1
0
150
100
50
nm
0
50
100
150

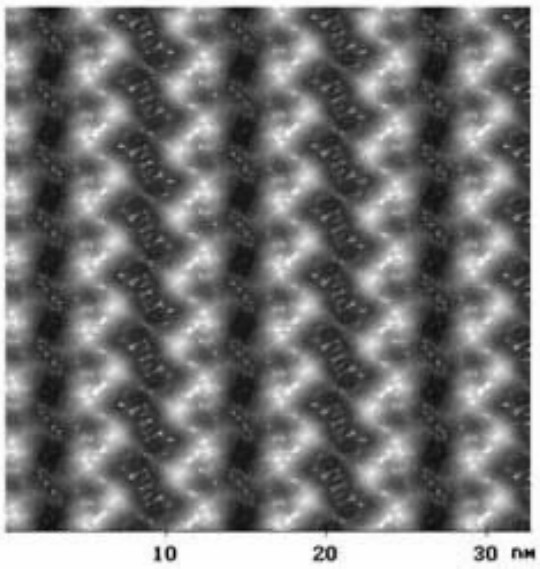

Experimental image

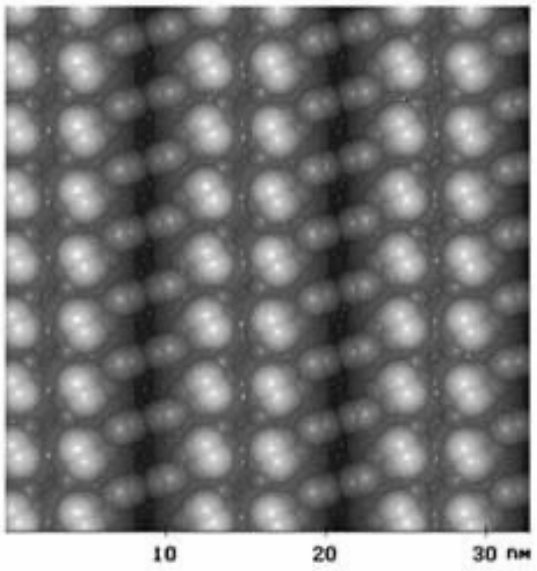

Theoretical image

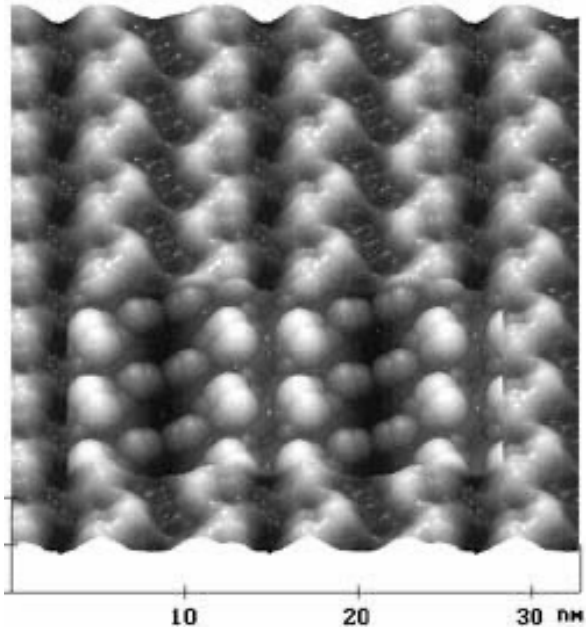

First hybrid image

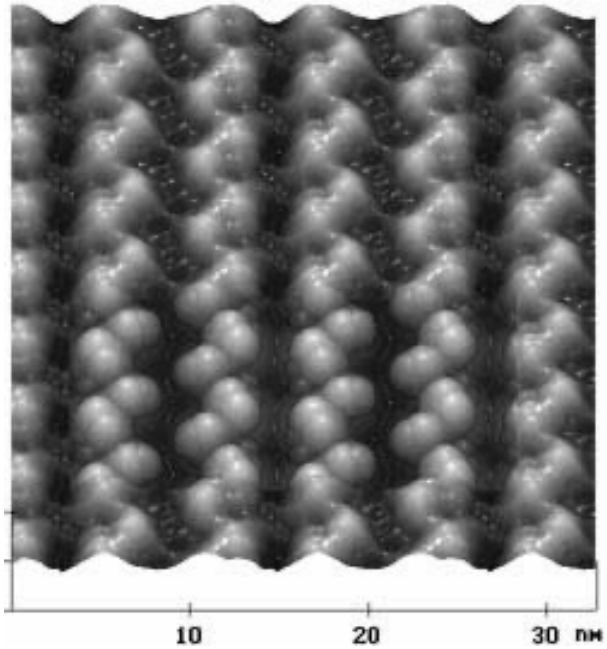

Revised hybrid image

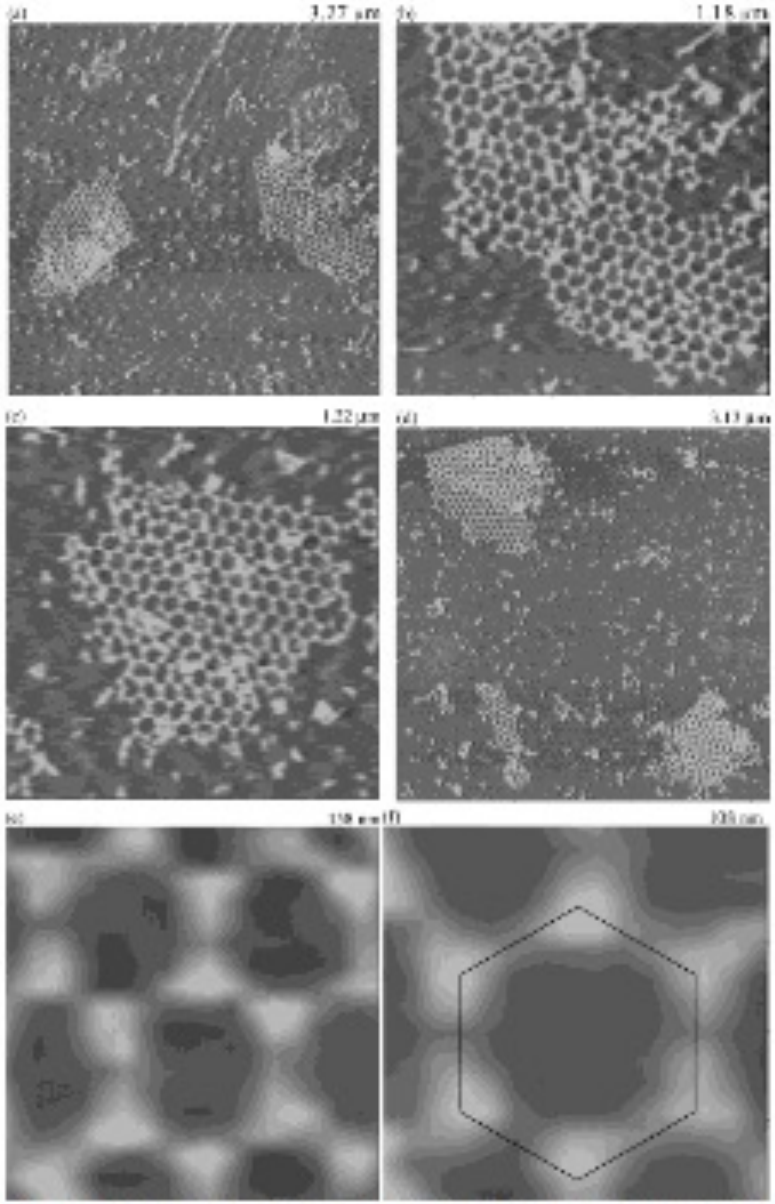

Figure 2. AFM images of pseudohexagonal trigonal arrays. Field sizes are indicated in the upper right corners. (a) A pair of 2D arrays. The honeycomb nature of the arrays are evident. (b) Zoom of the array on the right in (a). (c) Zoom of another array. (d) Image containing two stacked arrays, virtually complete on the lower right, partial on the upper left. (e) Zoomed image containing 15 DX triangles. (f) Further zoom of (e) showing six complete triangles, similar to the arrangement in 1d, and with a center−center hexagon superimposed.

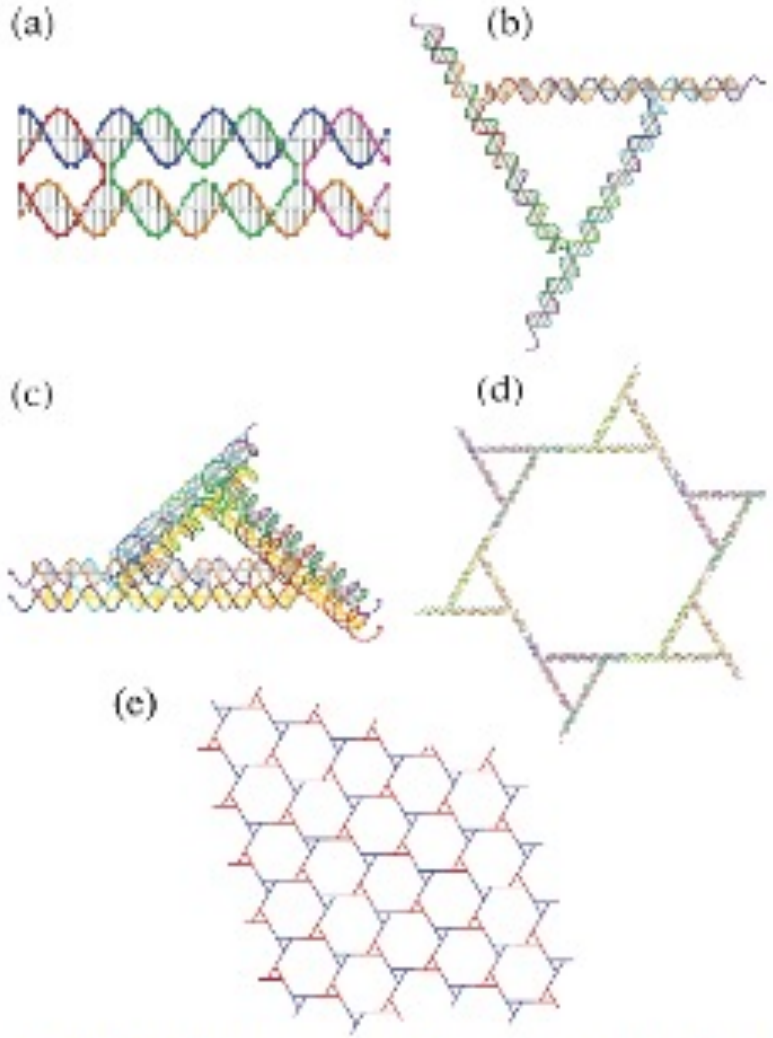

Figure 1. Motifs discussed here. (a) DX motif. (b) Bulged junction triangle. (c) DX triangle. (d) Trigonal arrangement of six DX triangles of two different species. (e) Schematic pseudohexagonal trigonal lattice of the two triangles.

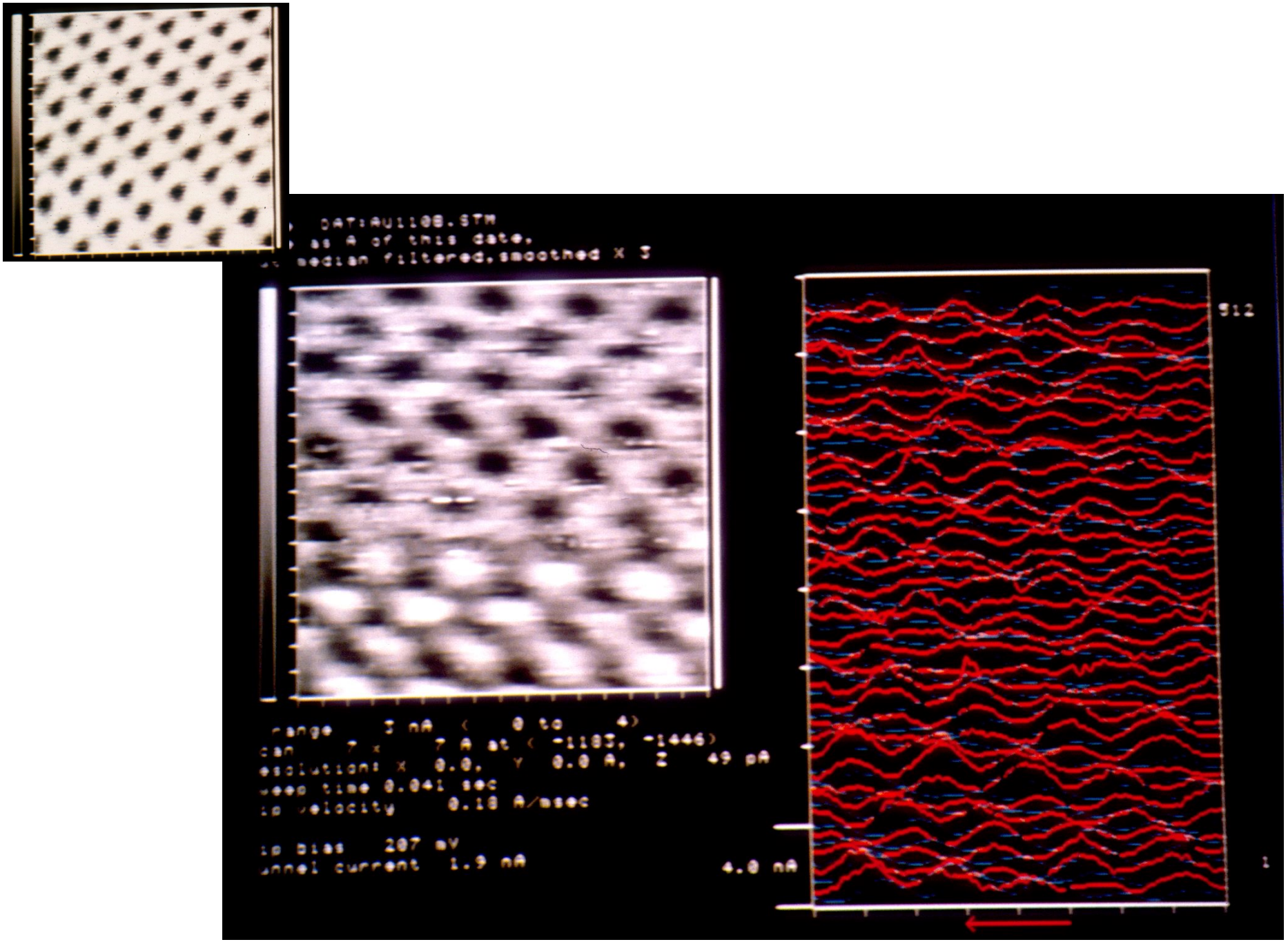
DAT:AU1108.STM
as A of this date,
median filtered,smoothed X I
range I nA (0 to 4)
912
4.0 nA
1

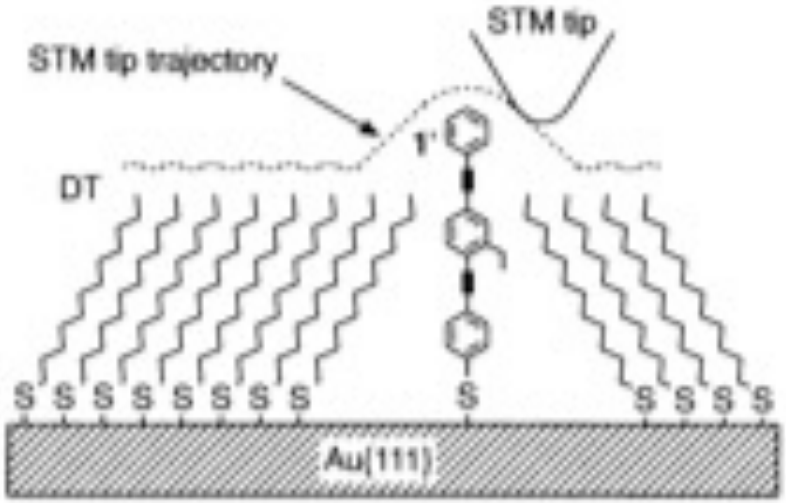
STM tip
STM tip trajectory
1'
DT
S S S S S S S S
S
S S S S
Au(111)

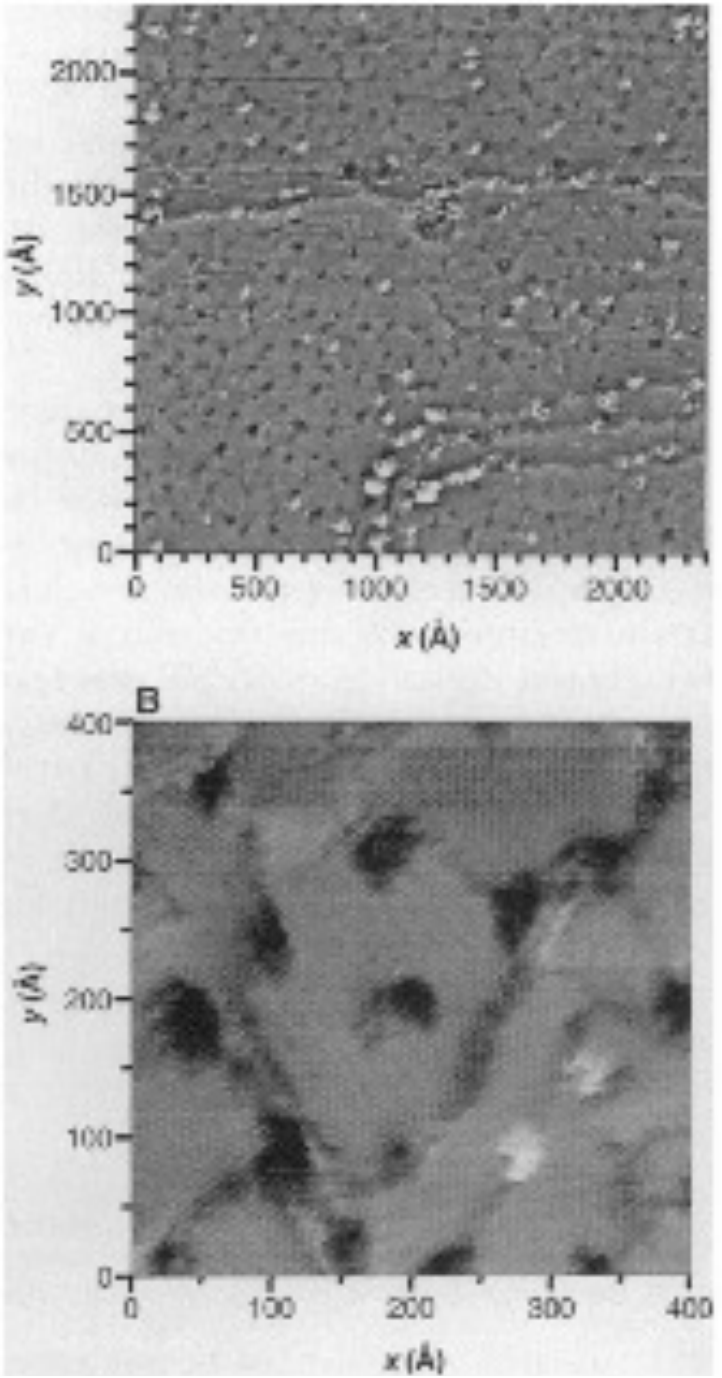
2000
1500
1000
500
0
y (Å)
0
500
1000
1500
2000
x (Å)
B
400
300
200
100
0
y (Å)
0
100
200
300
400
x (Å)


SCIENTIFIC AMERICAN
JUNE 2000
$4.95
www.sciam.com
Binding
THE BIRTH OF MOLECULAR ELECTRONICS
DWARF GALAXIES AND STARBURSTS
THE NETWORK INSIDE A CELL
SPECIAL REPORT: THE NEW FACE OF WAR
T
1
.S5

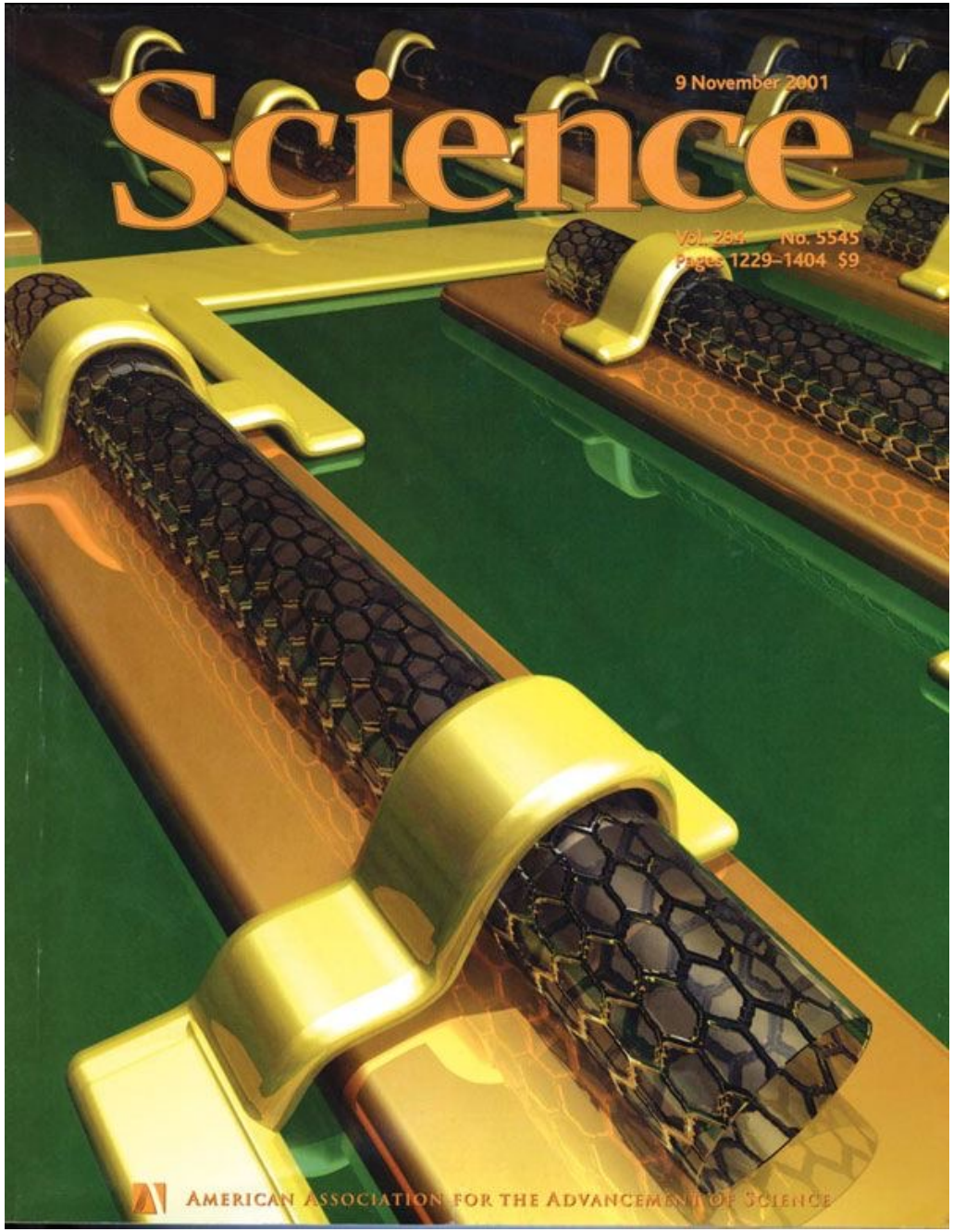
Science
9 November 2001
Vol. 284 No. 5545
Pages 1229–1404 $9
AMERICAN ASSOCIATION FOR THE ADVANCEMENT OF SCIENCE